RESTRICTED

NACA

RESEARCH MEMORANDUM

INVESTIGATIONS OF AIR-COOLED TURBINE ROTORS FOR TURBOJET ENGINES

II - MECHANICAL DESIGN, STRESS ANALYSIS, AND BURST TEST OF MODIFIED J33 SPLIT-DISK ROTOR

By Richard H. Kemp and Merland L. Moseson

Lewis Flight Propulsion Laboratory
Cleveland, Ohio

CLASSIFIED DOCUMENT

NATIONAL ADVISORY COMMITTEE FOR AERONAUTICS

WASHINGTON
January 14, 1952

RESTRICTED

NATIONAL ADVISORY COMMITTEE FOR AERONAUTICS

RESEARCH MEMORANDUM

INVESTIGATIONS OF AIR-COOLED TURBINE ROTORS FOR TURBOJET ENGINES

II - MECHANICAL DESIGN, STRESS ANALYSIS, AND BURST TEST OF MODIFIED J33 SPLIT-DISK ROTOR

By Richard H. Kemp and Merland L. Moseson

SUMMARY

As a part of an investigation instituted at the Lewis laboratory to apply turbine cooling to turbojet engines, a full-scale air-cooled rotor was designed, fabricated, and operated in a J33 turbojet engine.

Five basic rotor and cooling-air system designs were studied in order to determine a configuration which would be practical with respect to procurement, fabrication, and operation. The rotor design chosen for construction was of the split-disk type, providing for cooling-air induction in the center of the rear disk and passing the air radially outward through a vane system between the two disks to the base of each hollow air-cooled blade.

A stress analysis based on equal temperature distribution in both disks indicated that the rotor was structurally stable at rated engine conditions. Spin-pit testing of a similar rotor verified the analytical results. However, during operation of the rotor in a turbojet engine in a previous investigation, the rear disk maintained a temperature level substantially higher than that in the forward disk. The stress analysis was extended to take into account this temperature difference and the results indicated that excessively high stresses would be imposed on the forward disk and the serrations in the rim at rated engine conditions. Engine modifications are being made to permit the rotor to operate with both halves at approximately the same temperature level.

A comparison was made of the critical material content in the J33 production rotor and an air-cooled rotor of the same configuration.

INTRODUCTION

An investigation has been initiated at the NACA Lewis laboratory to extend the application of turbine cooling to full-scale turbojet engines thereby permitting a substantial reduction in the quantity of critical materials used in the turbine rotor. Prior investigations (references 1 to 7) demonstrate various methods of controlling the turbine-blade temperature distribution by air cooling. The present investigation, the heat transfer aspects of which are reported in reference 8, extends these techniques to the complete turbine rotor and examines the following attendant problems:

(1) Design of a stable rotor structure for supporting the air-cooled blades

(2) Provision for a cooling-air induction system to the rotor

(3) Supplying the cooling air to the blade bases with minimum aerodynamic and leakage losses

(4) Provision for equal distribution of the cooling air to all blades

(5) Producibility of the design and suitability for operation in conventional engines

The relative merits of five possible design configurations for air-cooled turbine rotors were considered and are discussed in terms of selection according to operational factors peculiar to each particular type of engine application. One of the five designs was selected for stress analysis, spin test, and engine operation to provide information on design techniques and operating difficulties, and an approximate indication of the potential reduction in the critical material content in turbine rotors made possible by air cooling.

The basis of the selection of the particular engine to be used for the initial application of air cooling to a full-scale engine was not considered very important because the results can be generalized. The J33 engine was readily available in a test setup and was used for the detailed study and experimentation reported herein.

TURBINE DESIGN CONSIDERATIONS

Introduction of cooling air and type of rotor structure. - A major consideration in developing the basic design configuration of an air-cooled turbine is the method of air introduction. In order to minimize cooling-air-flow losses, the air should be introduced at the smallest practical radius on the disk, where the tangential velocity is low.

Five possible methods for introducing cooling air into a turbine disk are presented schematically in figure 1. A split-disk rotor which introduces the cooling air through a hollow turbine shaft is illustrated in figure 1(a). In this design, the centrifugal blade loading is shared equally by two disks made as nearly symmetrical as possible. The torque produced by the turbine and any bending loads produced by disk vibration or flight conditions must be transmitted through the shaft connection to the forward disk. This design offers an attractive method of piping cooling air from the compressor discharge to the turbine rotor; however it is not practical where the amount of cooling necessary is so great that the use of large shafting is required which in turn may create serious bearing and weight problems. Major revisions would be required in order to adapt this cooling arrangement to current production engines.

A single disk carries all the blade loading and the cooling air enters from the center of the disk in the design illustrated in figure 1(b). A relatively light weight conical shroud attached to the rear surface of the turbine disk confines the cooling air enroute to the rim where it may be introduced directly to the blades through blade-base passages or, as illustrated, through holes in the rim of the disk connected with openings in the bottom of the blade bases. The shrouded-disk design results in a stress condition at the junction between the shaft and the disk more favorable than in the split-disk type, but has the following limitations: the method of attaining uniform cooling-air distribution to all blades is difficult; size and number of cooling-air passage holes through the rim of the disk are limited by stress considerations in the turbine disk; and reliable stress analysis techniques are lacking for the cooling-air shroud.

A cooling-air shroud applied to the forward side of the turbine disk is illustrated in figure 1(c). The considerations in the selection of this design are similar to those presented for figure 1(b) except that because the shroud is on the forward side of the disk, connections to the compressor discharge as a source of cooling air are more direct and the position of an air inlet seal is more easily maintained by locating it from the bearing housing rather than from the tail cone.

A split-disk design which introduces the cooling air through the rear disk is shown in figure 1(d) and another split-disk design in which the cooling-air inlet passes through the forward disk is shown in figure 1(e). The choice between bringing the cooling air through the forward or rear disk depends on the relative convenience of piping the cooling air from its supply source and sealing it at the entrance to the disk. The size of hole which can be tolerated in the center of the disk depends on the disk stress level. In some cases a hole large enough to introduce the necessary quantity of cooling air can be provided in the rear disk as in figure 1(d), but the larger hole required to give the same net flow area when the forward disk inlet of figure 1(e) is used results in excessive disk stresses.

No single optimum choice of type of rotor structure can be made from the five types presented, as the following factors could indicate any one of the five designs as being superior for a particular application: (1) quantity of cooling air required, (2) source of cooling air, (3) turbine diameter, (4) turbine speed and (5) power plant application. The split-disk design with cooling air introduced through the rear disk was determined to be the most feasible for the experimental air-cooled adaptation of the J33 engine, used in this investigation. For this application, emphasis was placed on achieving uniform cooling-air distribution to the blades within a wide range of cooling-air flow rates and on minimizing the extent of required alterations to an existing turbine design having a relatively high stress level in the rotor.

Cooling-air inlet seals. - The technique of effectively sealing the cooling air at the entrance to the turbine rotor constitutes a difficult and important problem. In a production model engine, air leakage at this point reduces engine efficiency and in an experimental model either substantially perfect sealing or a knowledge of the quantity of leakage is essential to obtain accurate heat-transfer data. Two sealing arrangements employing labyrinths as the sealing element are shown in figure 2. In both arrangements, the cooling-air supply tube is centered inside the labyrinth by means of pilot bearings to permit specification of small diametrical clearances between the labyrinth and the outside diameter of the air supply tube. The pilot bearing is located external to the air inlet tube in a labyrinth housing which is integral with the turbine disk (fig. 2(a)). In this arrangement the bearing is exposed to a relatively high temperature zone and its peripheral speed may, depending on the application, require external lubrication which in turn creates another difficult sealing problem. A reduction in the peripheral speed to a level permitting the use of grease-packed sealed pilot bearings may be accomplished by the arrangement shown in figure 2(b). In this arrangement, small pilot bearings are located inside the cooling-air supply tube on a spindle which is turned to be concentric with the main turbine-shaft bearings. The air inlet tube is centered by means of a four-vaned spider which is prevented from rotating by clips riveted to the inside of the air inlet tube. The tips of the vanes on the spider have a radius in the axial direction about a center on the spindle axis midway between the two pilot bearings to permit cocking of the air inlet tube. The maximum tip diameter of the spider forms a closer fit with the inside diameter of the air inlet tube than the fit between the labyrinth and the outside diameter of the tube. Another possible type of seal for this application is the face-contact type where rubbing contact occurs between the face of a stationary carbon ring and a mating surface on the rotating member. Operational experience with this type of seal at rubbing speeds in the region of 12,000 feet per minute has been limited to cases where a large amount of liquid cooling has been applied to the rubbing elements voiding its adaptability to this design in which no liquid is present.

Internal disk configuration. - The three basic objectives in designing the cooling-air passage configuration in a turbine disk are: (a) compression of the cooling air (b) uniform distribution of the cooling air to each of the turbine blades and (c) provision of good entrance flow conditions to the blades. The attainment of a proper velocity profile is complicated by the need for a relatively small distance between turbine disks or between a disk and a shroud and by the requirement that at the entrance to the blade base the passage be long in the axial direction and relatively narrow in the circumferential direction. Analysis indicated that the conditions of low tangential velocity, low cooling-air mass flow, and the inherent air passage shape limitations would not permit attainment of the first objective, (air compression) to any appreciable extent. Friction between the air and the disk surfaces might result in uniform cooling-air distribution, but analysis indicated it would be inadequate to achieve the tangential cooling-air velocity required to provide good entrance flow to the blades without vanes. A split-disk design employing 18 equally spaced sheet metal vanes to give tangential velocity to the air is shown in figure 3. The vanes are positioned between sheet metal faces on the inner surfaces of the disk and are supported by tabs projecting into slots in these sheet metal disks, bolts through bushings welded to the vanes, and mainly by the wedging action caused by diminishing passage thickness as the disk radius increased. Inasmuch as this design would not distribute cooling air equitably among the three blades of each group served by a single passage between vanes and required extreme care in sheet metal fabrication in order to form a reliable structure, it was not constructed. The design which was constructed and operated is described in the following section.

AIR-COOLED TURBINE

Turbine Rotor

General structure. - The split-disk design with cooling air introduced through the rear disk was chosen for initial construction of a full-scale air-cooled adaptation of the J33 engine (fig. 1(d)). The two halves of this rotor were clamped together by eighteen 7/16-inch diameter body-fit bolts (fig. 4), but the blade-base serrations provided the main restraint against relative radial displacement of the two disks.

The large diameter bore in the turbine shaft in the region of attachment to the forward disk was made in order to match, as closely as possible, the strengths of the two disks in the assembly. The small diameter hole in the center of the shaft was drilled through for thermocouple leads. The air inlet seal employed is of the type shown in figure 2(b) and was installed with the clearances indicated in figure 5.

Cooling-air passages. - Separate cooling-air passages for each blade to insure uniform distribution in the turbine rotor design are shown in figure 4. Although the vanes forming these passages were machined integral with the disks, the same rotor is adaptable to other vane configurations by machining out the present vanes and replacing them with a separate section of the rotor, containing vanes, to be clamped between the two existing disks.

Details of the 54 vanes may be seen more readily in the photograph (fig. 6) taken just after the disks were machined. This photograph shows how portions of the three inner blade fastening serrations were machined away to provide the cooling-air entrance passages to the blade bases. The clamping bolts protrude only slightly into the cooling-air passage because they are located in holes drilled through the vanes, as shown in figures 4 and 6.

Method of fabrication. - The time factor was a prime consideration in planning construction of the first full-scale air-cooled rotor in this investigation. In order, to save time on forging and to eliminate extensive machining operations including broaching the blade-root fastenings, a production model turbine disk was split into halves and the 54 air-cooling vanes were machined out of the exposed disk faces.

Although this procedure used a critical material (Timken 16-25-6 alloy), the investigation provided operating experience to determine structural characteristics of a split-disk design and measurements of radial and axial temperature distribution in the disk assembly. A total of 1/2-inch thickness in the axial direction was allowed for splitting the disk in the plane of rotation and for the subsequent finish machining to get flat and square faces on the surfaces of the disk which were clamped together. In addition to this 1/2-inch the over-all effective thickness of the disk was also reduced considerably by the cooling-air vanes machined in the disk. When the depths of the vanes in both disks are combined, a maximum depth of 0.75 inch at the root of the serrations and a minimum of 0.40 inch at all diameters between 8.50 inches and 11.62 inches are obtained. Because of the foregoing considerations, the original disk thickness was reduced at the rim from 2.80 inches to an effective thickness of 1.57 inches. All stress calculations, were made on this basis; the reductions in disk strength were partially compensated for by the reduced weight of the air-cooled blades.

In splitting the production model disk through the center in a plane perpendicular to its axis, a band saw was found to be almost completely ineffective and after one section of replaceable teeth in a large circular saw was broken, the disk was split by means of a lathe and a 3/8-inch-wide parting tool.

Tail Cone

In order to supply the cooling air to the disk at reasonable flow velocities, a maximum velocity at the entrance being approximately 400 feet per second, a flow area of 8.3 square inches was required in the cooling-air supply tubes. In order to prevent excessive heat addition to the cooling air by the exhaust gases of the engine, the interior of the tail-cone vanes could not be used directly for air passages and the arrangement shown in figure 7 was devised. The required flow area was provided by four $1\frac{5}{8}$-inch tubes entering the center section of the tail cone radially through a pair of redesigned, airfoil-shaped tail-cone vanes. This construction method provided an insulating air space between the inside of the tail-cone vanes and the air supply tubes and left the remaining two tail-cone vanes as they existed in the production engine. Since this tail cone was not a flight model, no attempt was made to achieve a light weight structure. The bellows located in the cooling-air inlet tube and the radial support on the disk side of the bellows were used to reduce the effect of thermal distortions of the tail-cone assembly on the axial position of the tube in the labyrinth in the turbine rotor. In order to provide an axial restraint for the air inlet tube, the inner tail-cone plate, located rearward of the turbine disk, was altered. The plate was given a deeper dish to clear the labyrinth air seal and was fitted loosely between lips of a two-piece ring at its enlarged central hole. This two-piece ring was threaded over the cooling-air inlet tube which could then be adjusted to anchor the inlet tube from the tail-cone plate in the proper axial position. Details of this anchor ring, which is shown in figure 7, can be seen in figure 5.

Turbine Blades

Airfoil section. - A hollow blade with a nine-tube pack insert was used with this turbine wheel. This blade profile was nontwisted and was of the same profile as blade 4 of reference 8. At the root section, this blade had the same profile as a production-model twisted blade for the same engine except that the leading-edge radius was approximately doubled. As in the rotor, no attempt was made to use noncritical materials for initial operation of the blades which were cast from X-40 alloy. The nine tubes, which were furnace brazed inside the shell, were of stainless steel. The size and location of the nine tubes in the pack are shown in figure 8. The wall thickness of the airfoil portion of the blade varied linearly from 0.060 inch at the root to 0.030 inch at the tip. This variation in wall thickness resulted in a ratio of total metal area, including the shell, tube pack, and braze metal, at the tip, to the metal area at the root of 0.61, as the tube pack and inner passage of blade were of constant cross section throughout the length of the blade.

Base section. - As shown in figure 8, the three lower serrations were omitted near the junction of the cooling-air passage in the wheel and the blade base. The cooling-air inlet passage in the base is an approximate airfoil and radially forms a transition to the airfoil shape of the inside of the blade section. A bulkhead was cast in the central portion of the cooling-air passage to increase the collapsing load that can be resisted by the blade base. The center of gravity of the blade in the axial direction was located over the parting line between the turbine disks and as a result of the 1/2-inch reduction in rim width, the trailing edge of the blade overhangs the blade base. A ledge was extended downstream on the top surface of the blade base to support the trailing edge (fig. 8).

Blade stress. - Since the tube pack in the shell was terminated at the top of the base, the root section of the shell carried the centrifugal load of the tube pack as well as the shell weight. The centers of gravity of the blade sections were stacked on a radial line and locating dimensions were given tolerances so that deviations would tend to compensate for gas-bending loads. The average tensile stress at the root of the shell due to centrifugal loading on shell, tube pack, and braze metal was 39,000 pounds per square inch at design speed of 11,500 rpm. Because metal temperatures were reduced by cooling, this stress level was considered tolerable. Stress level can be reduced 10,000 pounds per square inch by extending the brazed-tube packs into the base so that they will be partially self-supporting and by using larger tapers in the shell wall than those specified herein.

STRESS ANALYSIS OF ROTOR

Analysis Based on Similar Temperature Levels

Calculation method. - The stress analysis of the split-rotor design was initially performed by treating the two disks as independent rotating components. No restraining forces were assumed to be transmitted from one disk to the other, either through the bolts holding the two disks together or through the blade bases in the disk serrations. Since such conditions are probably desirable during engine operation of the rotor, special attention was given to those factors in the design which would influence relative deformations of the two disks. The profiles were made as nearly alike as was mechanically feasible to fulfill these conditions. The major difference between the two disks occurs at the center where a 3.25-inch diameter hole is necessary in the rear disk for induction of the cooling air while the forward disk is attached to the shaft. The end conditions were therefore made more nearly alike by boring a hole in the center of the forward disk and extending it into the shaft as shown in figure 4. Since the hole in the forward disk would not completely free the disk from restraint by the shaft, the major portion of the stress and burst analysis was devoted to the rear disk, which had no restraint at the hole.

For the purposes of the preliminary analysis, a predicted temperature gradient was used and was assumed to apply to both the forward and rear disks. Data were available from a previous study in which temperature measurements were made along the radius of a solid rotor operating in a turbojet engine similar to the one for which the air-cooled split rotor was designed. These temperature measurements at maximum operating speed were modified in accordance with the estimated effect of the cooling air passing through the rotor to the blades. The resulting assumed temperature variation along the radius of the disk which was used in the stress analysis is shown in figure 9. The temperatures are considered to be somewhat conservative since a very low cooling-air flow was assumed. Later in the investigation, actual temperature measurements were made of the split rotor during operation and were used in a more complete analysis which follows.

The general method of stress analysis which was employed is the finite-difference approach described in references 9 and 10 in which the elastic and the plastic conditions are treated for rotating disks with a temperature gradient. The variation of the properties of the disk material with temperature and the central hole for induction of the cooling air are taken into account in the analysis. The outside diameter of the disk is assumed to be the maximum diameter at which the disk is continuous in a circumferential direction. The entire serrated portion of the rim plus the turbine blade airfoil sections and turbine blade bases are considered as a uniformly distributed centrifugal load on the disk proper.

The internal cooling-air guide vanes provide an additional load distributed in a complex manner along the radius of the disk. These vanes were assumed to be nonsupporting and the load which they transmitted to the disk was assumed to be uniformly distributed in the tangential direction. This additional load on the disk was taken into account by increasing the density of the disk material at each point along the radius where the vanes exist by an amount equivalent to the weight of the vanes at that point.

This analysis produces the radial and tangential stresses along the radius of the rotor but does not take into account the presence of the 18 bolt holes near the rim of the rotor. Since the analysis shows that the tangential stresses at the bolt circle are nearly zero because of the combination of the effects of the centrifugal field and the thermal gradient, only the radial stresses need be considered in evaluating the stress concentration effects of the hole. If the small tangential stresses are neglected and the condition at the bolt circle is assumed to be one of tensile stress only, a stress concentration factor of approximately 2.8 (reference 11) would exist at the hole and would decrease very rapidly with distance from the hole in a tangential direction. For ordinary conditions of operation, the stress at the hole exceeds the elastic limit of the material and some plastic flow could be expected to occur.

The stress analysis was made at an overspeed of 12,650 rpm, which is 10 percent above maximum rated speed for the engine for which the split rotor was designed. The stresses at maximum rated speed, which is 11,500, are therefore approximately 20 percent below the stresses computed for the 10-percent overspeed. In addition, stress calculations were made at successively higher speeds and the diametral elongation was computed at each speed, taking into account plastic flow. A plot of the total diametral elongation against speed shows that at some speed the elongation increases very rapidly for small additional increases in speed. The curve reaches a maximum which defines the maximum attainable speed of the wheel. Previous experience has indicated that the experimental burst speed is 2 to 5 percent lower than the computed upper limit of the burst speed. The computed result is therefore modified accordingly to obtain a practical predicted burst speed.

Calculated stresses at 10-percent overspeed with assumed temperature gradient. - On the basis of the procedure described in the preceding section, a stress calculation was made for the rear disk at the 10-percent overspeed of 12,650 rpm based on the assumed temperature gradient shown in figure 9. The effective profile used in the calculation is shown in figure 10. "Effective profile" is used to differentiate between the plot of the effective disk thickness versus radius and the actual physical contour of the disk. The effective disk thickness versus radius is a faired curve which ignores projections and shoulders which carry no load, such as the cooling-air guide vanes. The load on the disk produced by these projections is taken into account by adjusting the density of the material at those points where the projections exist.

The diameter of the central hole indicated in figure 10 is 3.50 inches. The apparent discrepancy which exists between this value and the previously stated value of 3.25 inches is the result of a shoulder in the central hole of the disk which accomodates the cooling-air supply tube and provides a smooth entry for the air. The shoulder is not considered a part of the effective profile and hence the effective hole diameter is considered to be 3.50 inches.

The tangential and radial stress curves are shown below the effective profile in figure 10. The solid lines represent the results of a calculation in which the material was assumed to be completely elastic at all stress values. The dashed lines represent the results of a calculation in which plastic flow was assumed to occur in accordance with experimental stress-strain curves for the rotor material. The compressive tangential stresses at the rim are a result of the assumed temperature gradient along the disk radius. The elastic calculation shows high tangential stresses at the hole which are beyond the yield point of the material, which for the temperature near the hole is approximately 90,000 pounds per square inch. The manner in which these stresses are redistributed in the actual plastic case is illustrated by the dashed line. Only a small amount of plastic

flow is necessary to provide redistribution and does not constitute a hazardous condition. The radial stresses are zero at the hole, rise to a maximum of 62,000 pounds per square inch at a radial distance of 6.25 inches, and then drop to the rim-loading value of 26,000 pounds per square inch at the rim. The tangential stresses are nearly zero at the position of maximum radial stress.

In order to determine the loading effect of the cooling-air guide vanes on the disk, a second calculation was made in which the vanes were considered to be absent and all other factors were considered to be the same as in the first calculation. The results of the elastic calculation show that the cooling-air guide vanes increase the radial stresses approximately 2000 pounds per square inch at the maximum radial stress position and increase the tangential stress at the hole by approximately the same amount.

Serration shear stresses. - The shear stress existing in the serrations at 10-percent overspeed which is due to the action of the centrifugal force on the blades was calculated on the assumption of an even distribution of loading along all serrations and by use of a calculated value of 0.081 square inch of shear area per inch of individual serration length. On this basis, the shear stress was calculated to be 20,300 pounds per square inch. Only the top three serrations were assumed to carry the load since much of the bottom three is cut away to provide passage for the cooling air. The portion of the bottom three that remains is considered to be present only to prevent escape of the cooling air. The calculated shear stress is therefore somewhat conservative; however, it is seen that a substantial margin of safety exists when this value is compared with the shear rupture strength of the material. The tensile stress rupture for 16-25-6 alloy for 100 hours at 1000° F is approximately 83,000 pounds per square inch (reference 12). The shear rupture strength would be approximately 65 percent of this value or approximately 54,000 pounds per square inch. (The value of 65 percent was obtained from unpublished experimental data.)

Determination of theoretical burst speed. - As described previously, the elongation of the disk was computed at successively higher speeds until sufficient points were obtained for the plot shown in figure 11. The curve reaches a maximum at a speed of 17,900 rpm, which is therefore taken as the maximum attainable speed of the disk. It is apparent that a substantial factor of safety exists since the maximum operating speed is 11,500 rpm.

Spin-Pit Investigation

Purpose of spin test and description of rotor. - In the stress analysis of the split rotor just described, a number of assumptions were made to provide necessary simplification of the problem. In order

to test these assumptions and also since the split rotor was to be operated in a J33 turbojet engine, it was desirable to experimentally determine the burst strength of such a rotor to confirm the analytical results. A split rotor similar to the rotor intended for operation in the engine was therefore fabricated for the spin test. The cooling-air guide vanes were eliminated for the spin-test rotor to minimize the machining process. The calculations of the previous section provided substantial evidence that the effects of these vanes on the strength of the rotor would be small.

The profiles of the spin-test rotor were similar to the rotor intended for engine operation and the two disks were held together in the same manner, with eighteen $\frac{7}{16}$-inch bolts on a $13\frac{5}{8}$-inch bolt circle. The conditions at the center of the spin-test rotor were also similar to the engine rotor. A hole was machined in the rear disk and another was machined in the forward disk which extended into the shaft. A solid cone was machined and fastened to the rear disk in the cooling-air supply hole. This cone extended into the inner race of a bearing during operation with a clearance of approximately 1/8-inch between the cone and the inner race thus preventing excessive wobble and loss of the rotor during acceleration through the critical speeds. The spin test was performed in a vacuum with the rotor at room temperature.

Stress analysis. - A stress analysis of the spin-test rotor was made in a manner similar to that described in the preceding section for the rotor intended for engine operation. The rim loading was calculated to be 21,000 pounds per square inch at 12,650 rpm on the basis of a 150 gram airfoil plus its hollow base and the interrupted portion of the rotor at the rim. This value differs from the rim loading of the engine rotor because of a subsequent change in the design of the blade base. The loading was obtained through the use of ordinary solid blades which were cut to the proper length. The radial and tangential elastic stress curves are shown in figure 12 for 12,650 rpm together with the effective profile. Temperature along the radius was assumed to be constant. The tangential stress at the hole exceeds the elastic limit of the material by a small amount and some plastic flow would be expected giving a minor adjustment of stresses in the immediate vicinity of the hole. A prediction of the burst speed was made in the same manner as described previously and was determined to be 18,500 rpm. Since the actual burst speed is generally found to be 2 to 5 percent below the theoretical value, the rotor would be expected to burst in the range of approximately 17,600 to 18,100 rpm.

Spin test and burst test. - The forward and rear disks were assembled with short lengths of 0.005-inch piano wire placed between the two disks at the rim. Approximately 1 inch of wire was allowed to protrude from the rim. The eighteen 7/16-inch bolts holding the two

disks together were tightened to a prestress of 45,000 pounds per square inch and the rotor was spun to the 10 percent overspeed of 12,650 rpm. The correct prestress value was obtained by measurement of the bolt length. All the wires were still in position after this operation, indicating that the two disks had not separated at the rim.

Measurements were made of the rotor before and after running at various speeds. These measurements included (1) tip to tip of blades across a diameter, (2) diameter of bolt-hole circle for both disks, and (3) distance between disks near the center. These measurements were made with ordinary shop micrometers. Since the two disks touch each other only at the rim, the tightening of the bolts to the 45,000 pounds per square inch prestress produced a 0.021-inch movement of the two disks toward each other at the center. Operation at 12,650 rpm produced a further movement toward each other of approximately 0.003 inch. In order to interpret these dimensional changes, figure 13 illustrates the relative movement of the two disks at the center with variation in the bolt prestress. The three bolt prestresses used, 45,000, 30,000, and 15,000 pounds per square inch, were obtained by tightening to the corresponding bolt elongations. Measurements of the distance between the disks at the center were made at each prestress and these values are shown on the ordinate with the bolt prestress on the abscissa. As shown in figure 13, the bolt prestresses were set with sufficient accuracy and small changes in the bolting could cause relative disk movements of 0.003 inch in the axial direction. The change of 0.003 inch in the spacing between the disks due to operation at 12,650 rpm is therefore considered to be indicative of minor bolting changes rather than permanent deformation of the disks.

The measurements of the over-all diameter and the bolt-circle diameter before and after operation at 12,650 rpm indicated an increase of 0.003 inch. The accuracy of this measurement is questionable since no movement of the blades in the serrations in the case of the over-all diameter measurements and no motion of the tapered pins placed in the bolt heads for the bolt-circle measurements are assumed. Even if the entire 0.003 inch increase was attributed to permanent rotor deformation, it would not be serious since the spin test was made at a speed 10 percent above rated.

In order to determine the possibility of disk separation at the rim at reduced bolt tightness, the rotor was spun at 12,650 rpm at bolt prestresses of 30,000 and 15,000 pounds per square inch in addition to the initial value of 45,000 pounds per square inch. The runs were made without loss of any wires, indicating firm contact of the disks at the rim.

After the preliminary spin-test results were obtained, the rotor was spun to destruction, burst occurring at a speed of 17,200 rpm. The actual burst speed, therefore, compared favorably with the predicted range.

In figure 14(a) the forward disk is shown pieced together after the burst, with the shaft shown in the upper portion of the photograph. A view from the rear is presented in figure 14(b) and figure 14(c) shows the remaining fragments of the rear disk which do not appear in figure 14(b). The fracture lines are predominantly radial and no large rim sections were lost because of fracture lines between bolt holes, therefore bolt holes do not constitute a hazard in this design. Some of the radial fracture lines passed through the bolt holes while others did not. Approximately one-third of each of the two disks remained bolted together after the burst as shown in figure 14(b). The shaft fractured in the weld region.

Effect of Dissimilar Temperature Levels on Disk Stress Distribution

Measured temperature distribution. - In the foregoing analysis, the predicted temperature gradient shown in figure 9 was assumed to apply to both the forward and the rear disks of the split rotor. During operation of the split rotor in a J33 turbojet engine as described in reference 13, the forward disk ran at temperatures substantially lower than the rear disk. The estimated temperature distribution for the two disks at 11,500 rpm, effective gas temperature 1445° F, and effective cooling-air temperature 120° F at a coolant flow ratio of 0.02 is shown in figure 15 which was taken from reference 13. These temperature distributions were estimated from actual measured temperatures at lower speeds. A difference of approximately 375° F exists between the two disks. For the stress analysis of the disk proper, the curves are of interest only up to the 8-inch radius, beyond this point the temperatures are of interest in determining the strength of the blade fastening.

Elastic stress analysis at 11,500 rpm. - For the stress analysis, the disk material was assumed to remain elastic regardless of the magnitude of the stress. It was further assumed that the final position of the rim of the assembled rotor at 11,500 rpm would be halfway between the positions of the rims of the individual disks if allowed to elongate without restraint. This assumption implies equal radial stiffness of the two disks and also implies perfect transmission of the restraining forces from one disk to the other through the blade bases in the rotor serrations. Evidently a certain amount of relative motion of the two disks could actually occur without transmission of restraining forces because of the small clearances between the blade and the rotor serrations.

The total radial elongations of the two disks, treated as free bodies rotating at 11,500 rpm, were calculated to be 0.040 inch for the rear disk and 0.013 inch for the forward disk. The restraining force which would be required to produce a total radial elongation of 1/2 the difference between the elongations (0.040-0.013) or 0.0135 inch in each

disk was then calculated and found to be 73,800 pounds per square inch. The total effective rim loading on the forward disk was therefore 21,660 pounds per square inch (the rim loading produced by the blades and the interrupted portion of the disk) plus the tensile restraining load of 73,800 pounds per square inch or 95,460 pounds per square inch. In the case of the rear disk the restraining load is compressible so that the total effective rim loading is therefore 21,660 minus 73,800 or -52,140 pounds per square inch. The elastic stress analysis was then made for each disk at the speed of 11,500 rpm using the appropriate total effective rim loading and the results are shown in figure 16. The tangential and radial stresses for the rear disk are entirely compressive because of the effective rim loading of -52,140 pounds per square inch. The forward disk on the other hand has very high tensile stresses because of the high positive rim loading of 95,460 pounds per square inch. Although the disk material was assumed to be elastic for all stress values, actually the elastic limit is exceeded in the forward disk. For this reason, a more rigorous approach was utilized, taking into account the plastic flow of the material in the disks.

Plastic stress analysis at 11,500 and 14,500 rpm. - Because of plastic flow, the rim of the assembled rotor could no longer be assumed to seek a position at 11,500 rpm midway between the positions of the rims of the two disks treated as independent bodies. In order to obtain the total effective rim loading, it was necessary to employ a more elaborate procedure. Various values of restraining load were assumed and the total radial elongation of each disk was calculated for plastic flow for each assumed restraining load plus the normal rim loading. The elongation was plotted against restraining load for each disk and is shown in figure 17. Since it is assumed that the radial elongations of the two disks must be equal because of the connection at the rim, the restraining load is determined by the point at which the elongation curves intersect. The restraining load at the speed of 11,500 rpm is 50,000 pounds per square inch (fig. 17). The total effective rim loading on the forward disk is then 21,660 plus 50,000 or 71,660 pounds per square inch and the total effective rim loading on the rear disk is 21,660 minus 50,000 or -28,340 pounds per square inch.

By utilization of the computed total effective rim loadings, the tangential and radial stresses were calculated for plastic flow and the data shown in figure 18. The stresses in the forward disk are considerably lower as a result of the plastic flow than in the analysis in which complete elasticity was assumed. In order to obtain some indication of the imminence of rotor failure, another plastic analysis was made at a speed of 14,500 rpm in the same manner as that described for 11,500 rpm. The elongation versus restraining load curves are shown in figure 17. At 14,500 rpm the elongations of the two disks are equal at a restraining load of 29,000 pounds per square inch. The total effective rim loadings are therefore 34,430 pounds per square inch (rim loading caused

by blades and interrupted portion of disks) plus 29,000 pounds per square inch or 63,430 pounds per square inch for the forward disk and 34,430 minus 29,000 or 5,430 pounds per square inch for the rear disk. By utilizing these computed effective rim loadings, the stresses were again calculated for plastic flow and are shown in figure 19. A comparison of the results at 14,500 rpm with those of figure 18 for 11,500 rpm shows that the increase of 3000 rpm produced only a small change in the stresses in the forward disk but substantially increased the stresses in the rear disk. The processes involved are therefore evident. At the lower speeds of rotation, the high restraining loadings that result from the differential thermal expansions produce high tensile stresses in the forward disk and very low or compressive stresses in the rear disk. As rotative speed is increased, the stresses in the forward disk exceed the elastic limit of the material, resulting in plastic flow. This plastic flow, as shown in figure 17 reduces the restraining load and increases the effective rim loading on the rear disk while decreasing the effective rim loading on the forward disk. The stresses in the forward disk change only a small amount as a result of the combination of reduced restraining loading and increased speed while the stresses in the rear disk increase rapidly. A certain speed is reached at which the plastic flow decreases the restraining load to zero and both disks then attain the same stress levels. Although the forward disk attains a high stress level at operating speeds, the condition is not necessarily hazardous since a small amount of plastic flow in effect unloads the forward disk and causes the rear disk to assume more of the rim loading.

Effect of rotor serrations and strength of blade fastening. - In this analysis, the two disks were assumed to be rigidly fastened together, thereby permitting no relative motion of the disks at the rim. This assumption is not strictly correct, since some relative motion could occur as a result of the clearances of the blade bases in the rotor serrations. This relative motion would reduce the restraining forces to some extent by permitting the rear disk to expand slightly before applying forces to the forward disk. The magnitude of the relative motion which materially reduces the restraining load is indicated in figure 17. The elongation curves for 11,500 rpm show that a difference of 0.010 inch in radial elongation of the two disks reduces the restraining load to only 41,000 pounds per square inch.

The analysis described in the foregoing sections has been concerned only with the rotor proper and the assumption has been made that the restraining forces can be transmitted through the blade bases in the disk serrations without distortion or rupture of the serrations. The restraining forces are assumed to be transmitted in a uniformly distributed manner. Any attempt to estimate the stresses in the serrations caused by the restraining forces and the centrifugal load of the turbine blades must take into account the fact that the loading imposed on the

serrations is not simple nor uniformly distributed. By expanding relative to the forward disk, the rear disk actually causes a system of bending moments to be set up in the serrations. In addition to this system of bending moments, the centrifugal forces of the turbine blades are distributed in some unknown manner over the serrations. A rigorous analysis of this complex load distribution was not attempted. However, to obtain some idea of the magnitude of the serration shear stresses, a calculation was made on the basis of a uniform load distribution at the speed of 11,500 rpm which indicated a serration shear stress of 64,400 pounds per square inch. The high indicated serration shear stresses and the high disk stresses demonstrate that it is necessary to reduce the temperature difference between the two disks to permit satisfactory operation of the rotor in the engine.

EFFECT ON CRITICAL MATERIALS REQUIRED

Direct substitution of a noncritical material in blades and disks of the same configuration as the air-cooled split-disk rotor discussed herein was investigated. Stress analysis based on the radial temperature gradients plotted on figure 15 for the forward and rear disks indicated that Timken 17-22A(S) had sufficient strength for this disk application. The same material also exhibited adequate strength when used for the rotor blades during the engine cyclic tests reported in reference 14. A comparison of weights and critical material content between an air-cooled turbine rotor of the same configuration as that reported and the J33 engine is presented in table I. A reduction in total rotor weight of 46.2 percent as indicated in the table would not be likely generally because this air-cooled rotor is compared with an obsolete model non-cooled design which is much heavier than the current production rotor for the same engine. Because reductions up to 98 percent can be accomplished in the critical material content of turbine blades and disks for operation at present gas temperatures of 1600° F to 1700° F, the use of intermediate alloys in conjunction with air cooling could increase these gas temperatures.

SUMMARY OF RESULTS

An air-cooled split-disk turbine rotor having a set of hollow blades with a nine-tube pack insert and a modified engine tail cone was designed for experimental operation in a J33 turbojet engine. The design was chosen on the basis of a study of five basic rotor and cooling-air system configurations. The rotor design was of the split-disk type, providing for cooling-air induction in the center of the rear disk and passing the air radially outward through a vane system between the two disks to the base of each hollow air-cooled blade.

A stress analysis was made of the split-disk rotor having cooling-air induction in the rear face, utilizing a predicted temperature gradient which was assumed to apply to both the forward and rear disks. This analysis indicated that the air-cooled rotor was structurally sound and capable of operation at rated engine conditions.

Another rotor of the same configuration as the engine rotor except for omission of the cooling-air guide vanes was constructed for spin test as a check on the analytical procedure. Spinning at an overspeed of 10 percent above rated showed the rotor to be free from any undesirable permanent deformations. The spin test was continued to burst which occurred at 17,200 rpm. The predicted range of burst was 17,600 to 18,100 rpm.

Operation of the split-disk rotor in the J33 turbojet engine at speeds up to 600 rpm showed that the two disks did not operate at the same temperature levels. Data extrapolated to rated speed conditions indicated a temperature difference between the two disks of approximately 375° F. For this reason, a second stress analysis was made utilizing the new temperature distribution curves. This analysis showed that high stresses were imposed on the forward disk as a result of the greater elongation of the rear disk and consequent transmittal of restraining forces through the blade bases in the disk serration. In addition to the undesirable disk stresses the analysis indicated that the stresses in the serrations were beyond safe operating levels. The assumption was made in this analysis that perfect transmittal of the restraining forces was obtained through the blade bases. The computed disk stresses are therefore somewhat conservative since some motion of the bases in the serrations due to clearances would tend to reduce the restraining forces. However, the analysis indicated that definite measures should be taken to permit operation of the split-disk rotor in the engine at substantially the same temperatures in the two disks.

Results indicated that a substitution of a noncritical material could be made in both the disks and the blades. The reduction in critical material content amounted to approximately 98 percent in a comparison based on use of Timken 17-22A(S) in the air-cooled rotor reported and the J33 engine.

Lewis Flight Propulsion Laboratory
National Advisory Committee for Aeronautics
Cleveland, Ohio

REFERENCES

1. Ellerbrock, Herman H., Jr., and Stepka, Francis S.: Experimental Investigation of Air-Cooled Turbine Blades in Turbojet Engine. I - Rotor Blades with 10 Tubes in Cooling-Air Passages. NACA RM E50I04, 1950.

2. Hickel, Robert O., and Ellerbrock, Herman H., Jr.: Experimental Investigation of Air-Cooled Turbine Blades in Turbojet Engine. II - Rotor Blades with 15 Fins in Cooling-Air Passages. NACA RM E50I14, 1950.

3. Hickel, Robert O., and Smith, Gordon T.: Experimental Investigation of Air-Cooled Turbine Blades in Turbojet Engine. III - Rotor Blades with 34 Steel Tubes in Cooling-Air Passages. NACA RM E50J06, 1950.

4. Ellerbrock, Herman H., Jr., Zalabak, Charles F., and Smith, Gordon T.: Experimental Investigation of Air-Cooled Turbine Blades in Turbojet Engine. IV - Effects of Special Leading- and Trailing-Edge Modifications on Blade Temperature. NACA RM E51A19, 1951.

5. Smith, Gordon T., and Hickel, Robert O.: Experimental Investigation of Air-Cooled Turbine Blades in Turbojet Engine. V - Rotor Blades with Split Trailing Edges. NACA RM E51A22, 1951.

6. Arne, Vernon L., and Esgar, Jack B.: Experimental Investigation of Air-Cooled Turbine Blades in Turbojet Engine. VI - Conduction of Film Cooling of Leading and Trailing Edges of Rotor Blades. NACA RM E51C29, 1951.

7. Smith, Gordon T., and Hickel, Robert O.: Experimental Investigation of Air-Cooled Turbine Blades in Turbojet Engine. VIII - Rotor Blades with Capped Leading Edges. NACA RM E51H14, 1951.

8. Ellerbrock, Herman H., Jr., Zalabak, Charles F., and Smith, Gordon T.: Experimental Investigation of Air-Cooled Turbine Blades in Turbojet Engine. IV - Effects of Special Leading- and Trailing-Edge Modifications on Blade Temperature. NACA RM E51A19, 1951.

9. Manson, S. S.: Analysis of Rotating Disks of Arbitrary Contour and Radial Temperature Distribution in the Region of Plastic Deformation. Paper presented at the First U. S. National Congress of Applied Mechanics (Chicago), June 11-16, 1951.

10. Manson, S. S.: Direct Method of Design and Stress Analysis of Rotating Disks With Temperature Gradient. NACA Rep. 952, 1950. (Formerly NACA TN 1957.)

11. Maleev, V. L.: Machine Design. International Textbook Co., 1939, pp. 34-36.

12. Fleischmann, Martin: 16-25-6 Alloy for Gas Turbines. Iron Age, vol. 157, no. 3, Jan. 17, 1946, pp. 44-53; cont., vol. 157, no. 4, Jan. 24, 1946, pp. 50-60.

13. Schramm, Wilson B., and Ziemer, Robert R.: Investigations of Air-Cooled Turbine Rotors for Turbojet Engines. I - Experimental Disk Temperature Distribution in Modified J33 Split-Disk Rotor at Speeds up to 6000 RPM. NACA RM E51I11, 1952.

14. Stepka, Francis S., and Hickel, Robert O.: Experimental Investigation of Air-Cooled Turbine Blades in Turbojet Engine. IX - Evaluation of the Durability of Noncritical Rotor Blades in Engine Operation. NACA RM E51J10, 1951.

2346

TABLE I - COMPARISON OF WEIGHTS AND CRITICAL MATERIAL CONTENT BETWEEN AIR-COOLED SPLIT ROTOR OF *REDUCED CRITICAL MATERIAL CONTENT AND ORIGINAL NONCOOLED ROTOR*

[Timken 17-22A(S) assumed in noncritical rotor and blades, Timken 16-25-6 in original turbine rotor, and S-816 in original blades.]

Unit	Type of unit	Unit weight (lb)	Weight reduction in air-cooled design (percent)	Critical material content (lb)							Critical material content reduction in air-cooled design (percent)
				Cb	Co	W	Cr	Mo	Ni	V	
Rotor assembly, turbine rotor and blade without shaft	Air-cooled noncritical design	146.6	46.2				1.83	0.73		0.37	98.1
	Original noncooled design	272.0		1.77	19.82	1.99	45.30	15.51	65.70		
Turbine rotor without blades or shaft	Air-cooled noncritical design	115.2	48.8				1.44	0.57		0.29	97.8
	Original noncooled design	225.0					36.00	13.50	56.25		
Complete set of 54 turbine blades	Air-cooled noncritical design	31.4	33.0				0.40	0.15		0.08	98.6
	Original noncooled design	46.9		1.77	19.82	1.99	9.29	2.010	9.45		
Base portion of single blade	Air-cooled noncritical design	0.254	38.6				0.0032	0.0013		0.0006	98.7
	Original noncooled design	0.414		0.0156	0.1750	0.0176	0.0821	0.0178	0.0835		
Airfoil portion of single blade	Air-cooled noncritical design	0.327	28.0				0.0041	0.0016		0.0008	98.5
	Original noncooled design	0.454		0.0171	0.1920	0.0193	0.0901	0.0195	0.0916		

Chemical composition

Material	C	Mn	P	S	Si	Cr	Mo	V	Ni	N	Co	W	Cb
17-22A(S)	0.28-0.33	0.45-0.65	0.040 max	0.040 max	0.55-0.75	1.0-1.5	0.40-0.60	0.20-0.30	--------	--------	-----	----	----
16-25-6	.08-.10	2.0 max	---------	---------	1.0 max	16.0	6.0	--------	25.0	0.15	-----	----	----
S-816	.38	.49	---------	---------	.39	19.84	4.30	--------	20.17	--------	42.28	4.26	3.77

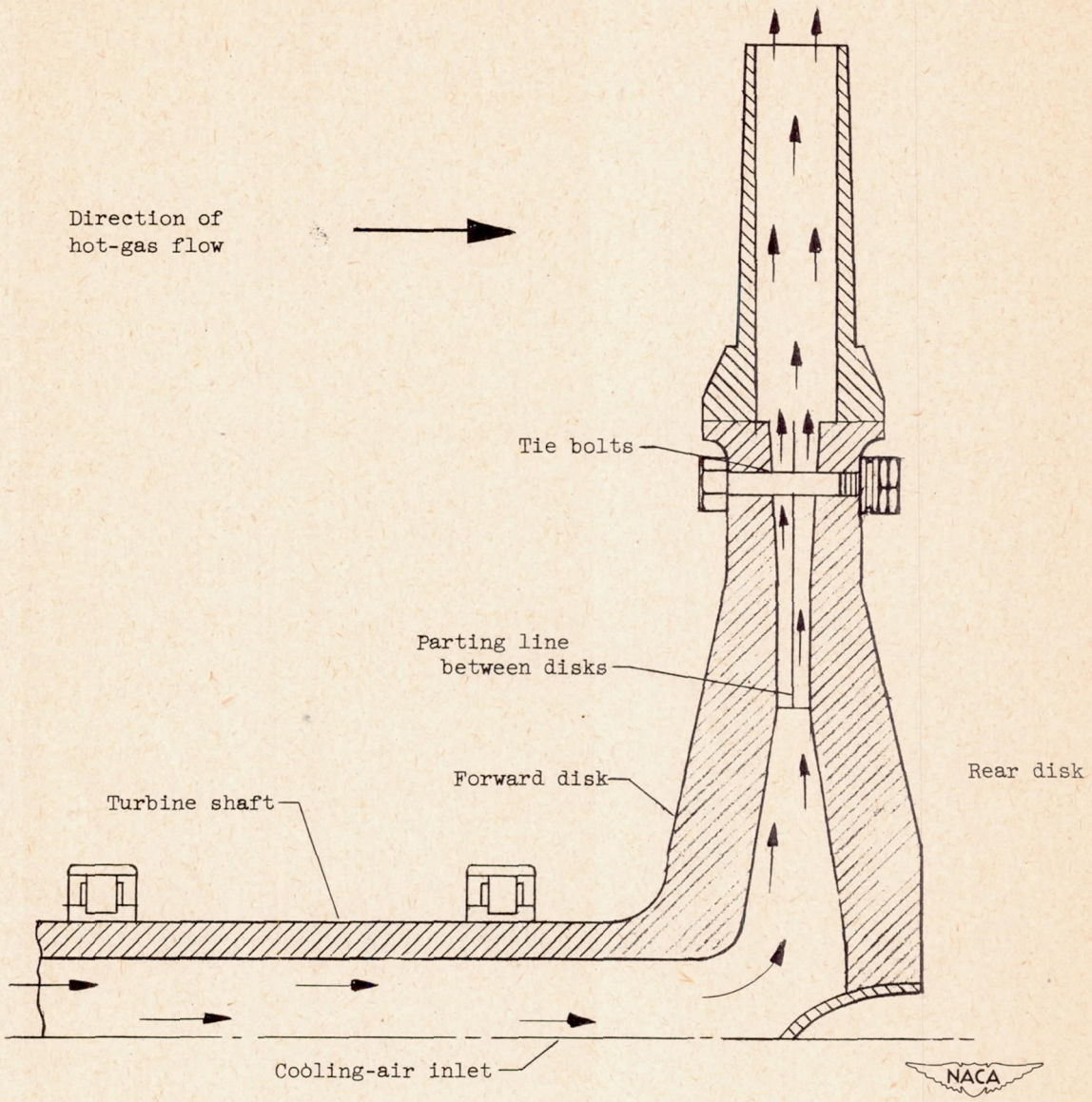

(a) Split-rotor with cooling-air inlet through hollow turbine shaft.

Figure 1. - Five alternative configurations for cooling turbine rotors and blades using light weight conical shrouds and split rotors as basic structures.

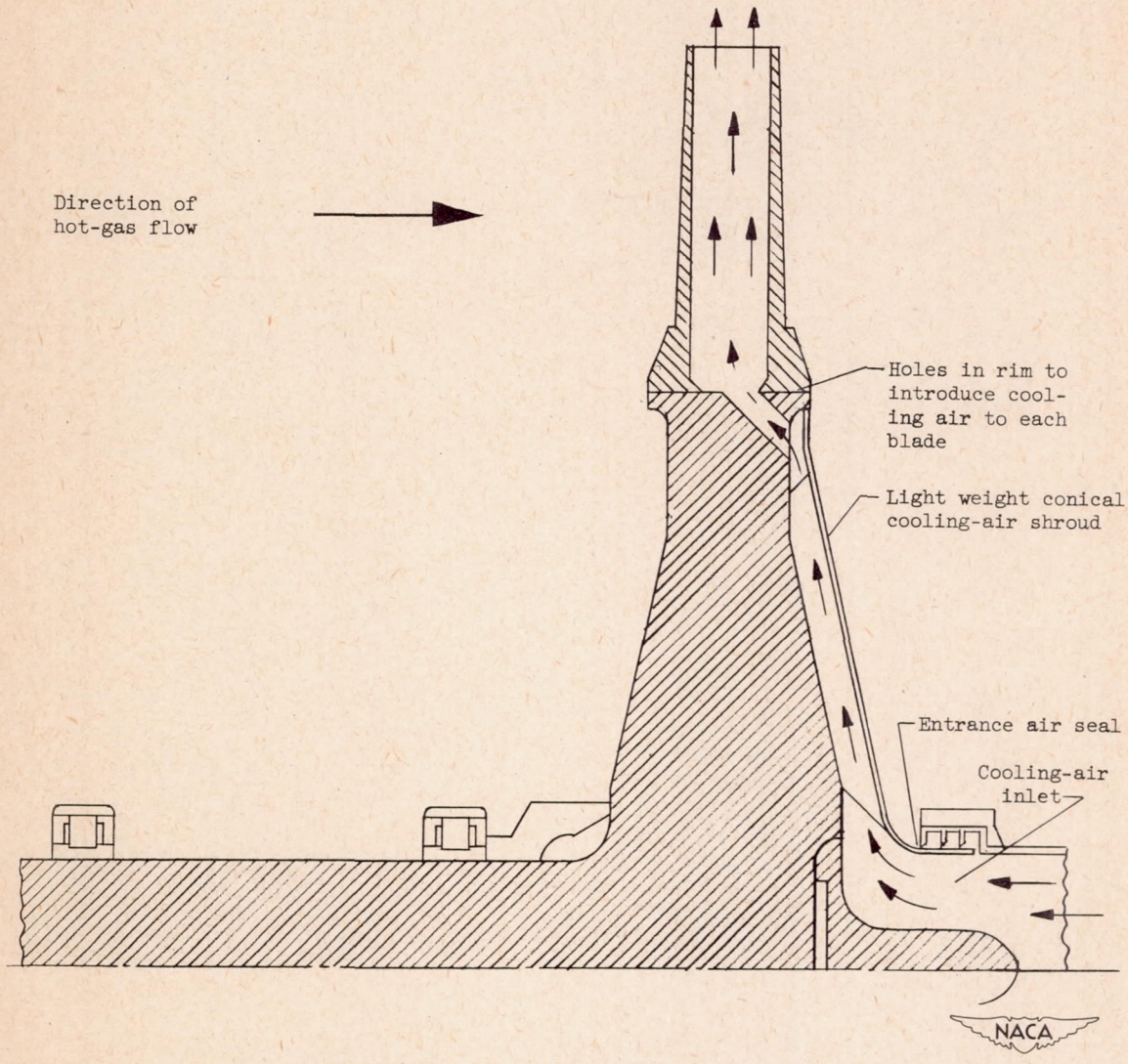

(b) Light weight cooling-air shroud on rear face of rotor.

Figure 1. - Continued. Five alternative configurations for cooling turbine rotors and blades using light weight conical shrouds and split rotors as basic structures.

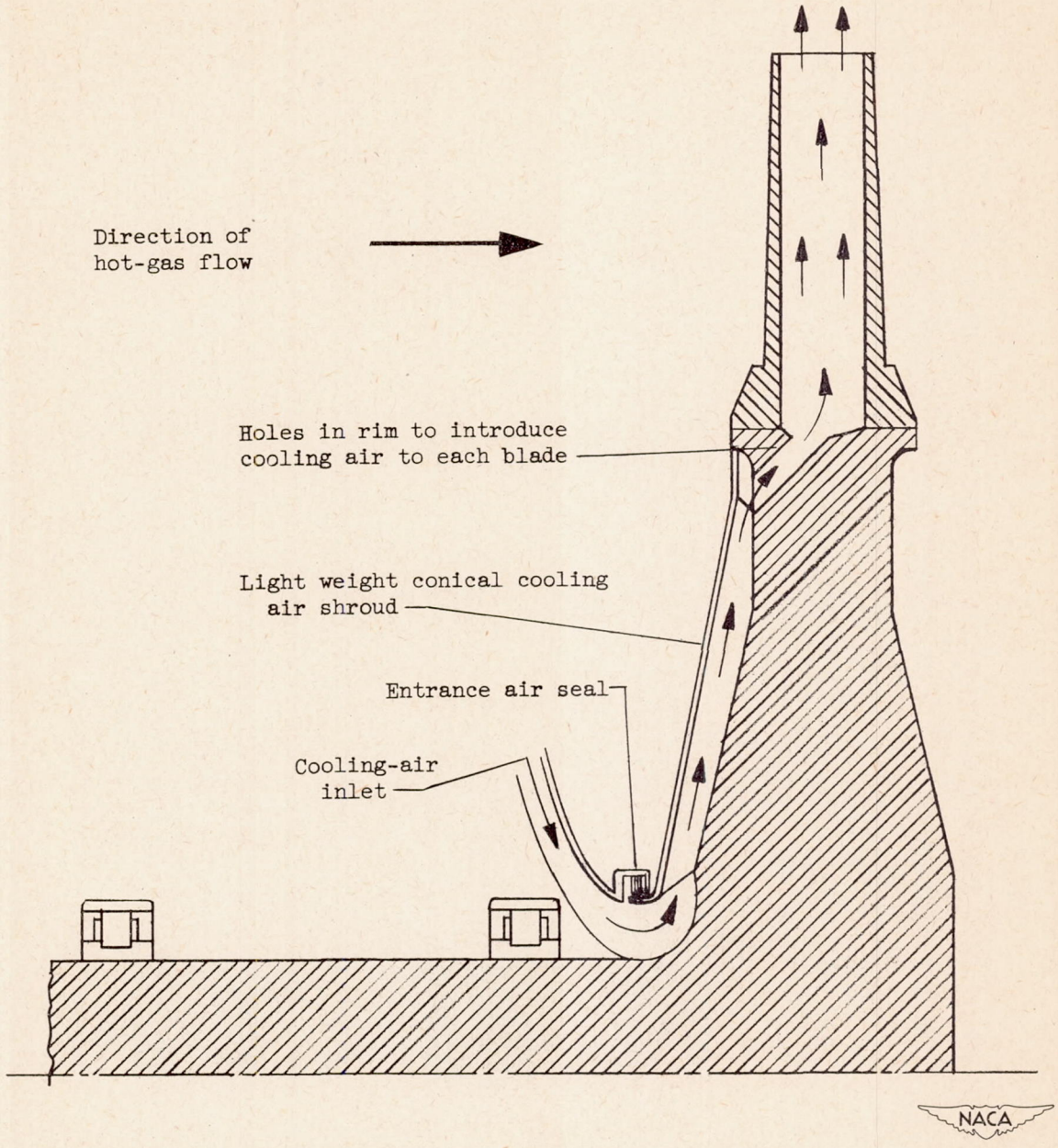

(c) Light weight cooling-air shroud on forward face of rotor.

Figure 1. - Continued. Five alternative configurations for cooling turbine rotors and blades using light weight conical shrouds and split rotors as basic structures.

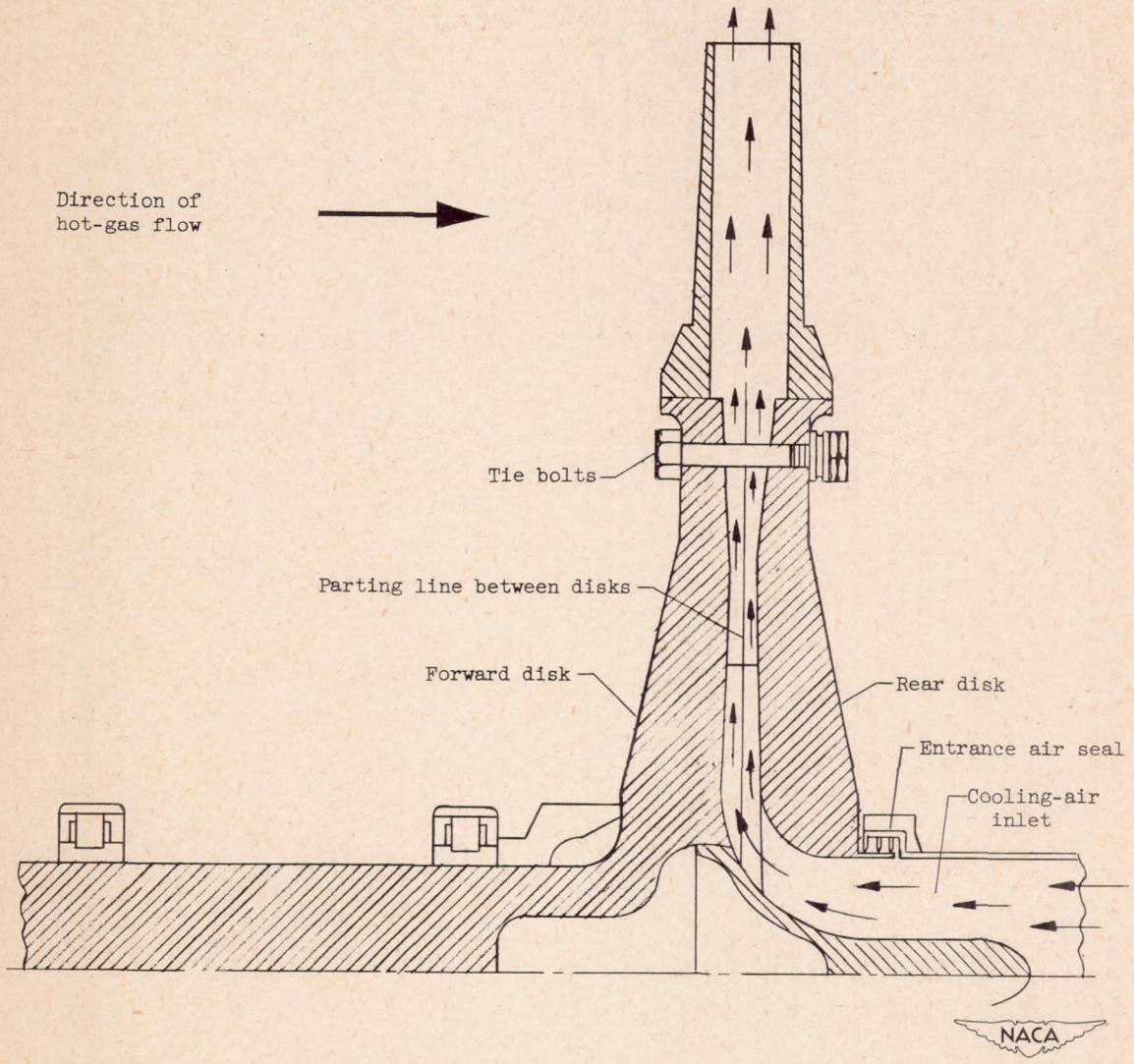

(d) Split-rotor for air cooling with rear cooling-air inlet.

Figure 1. - Continued. Five alternative configurations for cooling turbine rotors and blades using light weight conical shrouds and split rotors as basic structures.

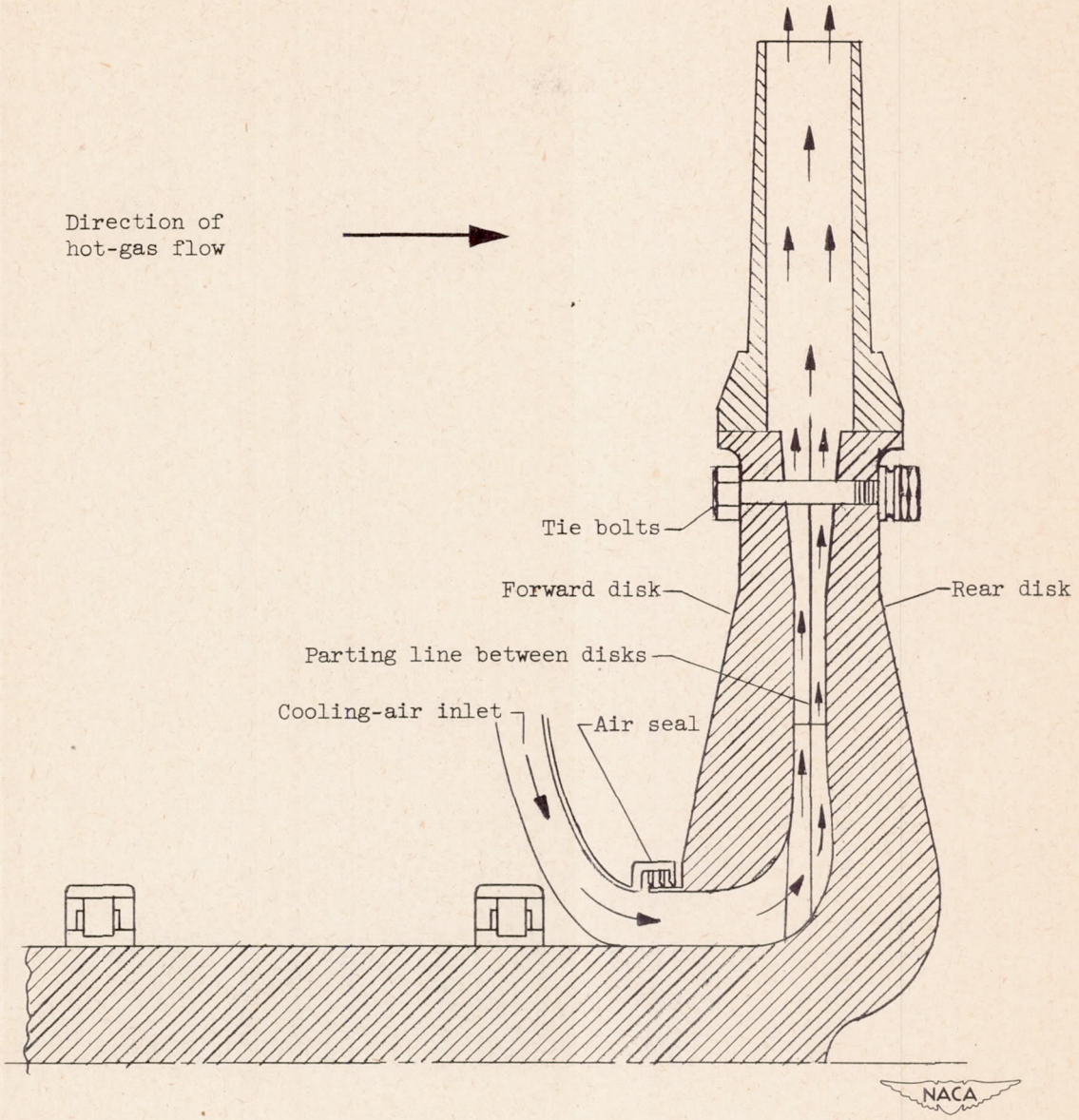

(e) Split-rotor for air cooling with forward cooling-air inlet.

Figure 1. - Concluded. Five alternative configurations for cooling turbine rotors and blades using light weight conical shrouds and split rotors as basic structures.

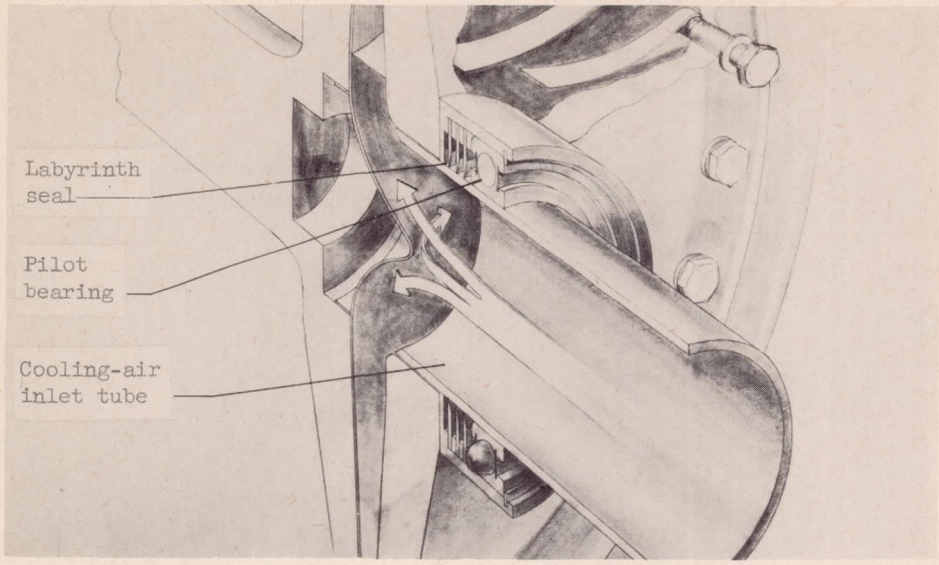

(a) Pilot bearing in labyrinth seal housing mounted on outside diameter of air inlet tube.

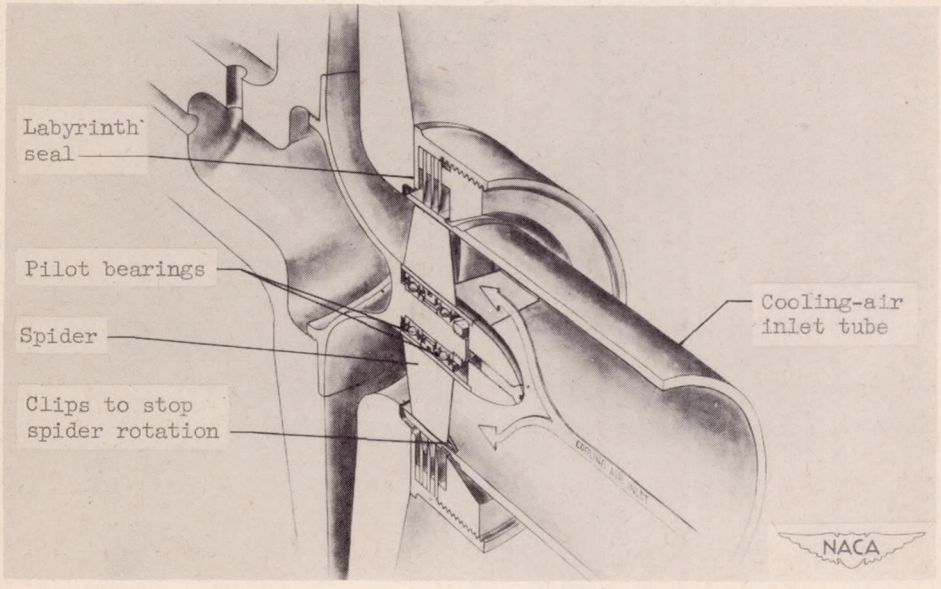

(b) Pilot bearing located on spindle attached to turbine disk and centering air inlet tube by means of four vane spider.

Figure 2. - Alternative arrangements for maintaining cooling-air inlet tube concentric with air seal labyrinths attached to rotor for rear-disk cooling-air inlet.

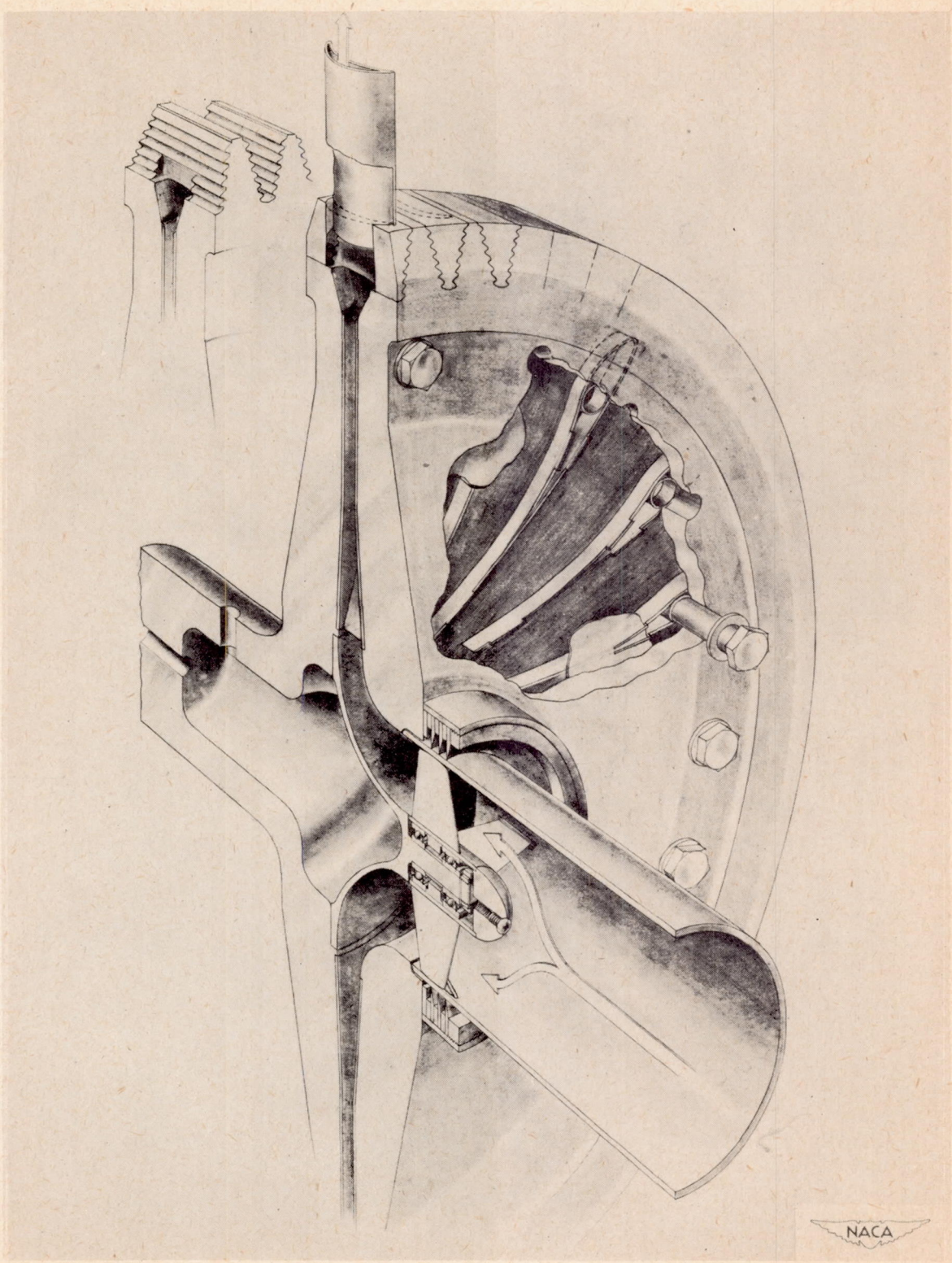

Figure 3. - Proposed air-cooled split-rotor with 18 sheet metal vanes.

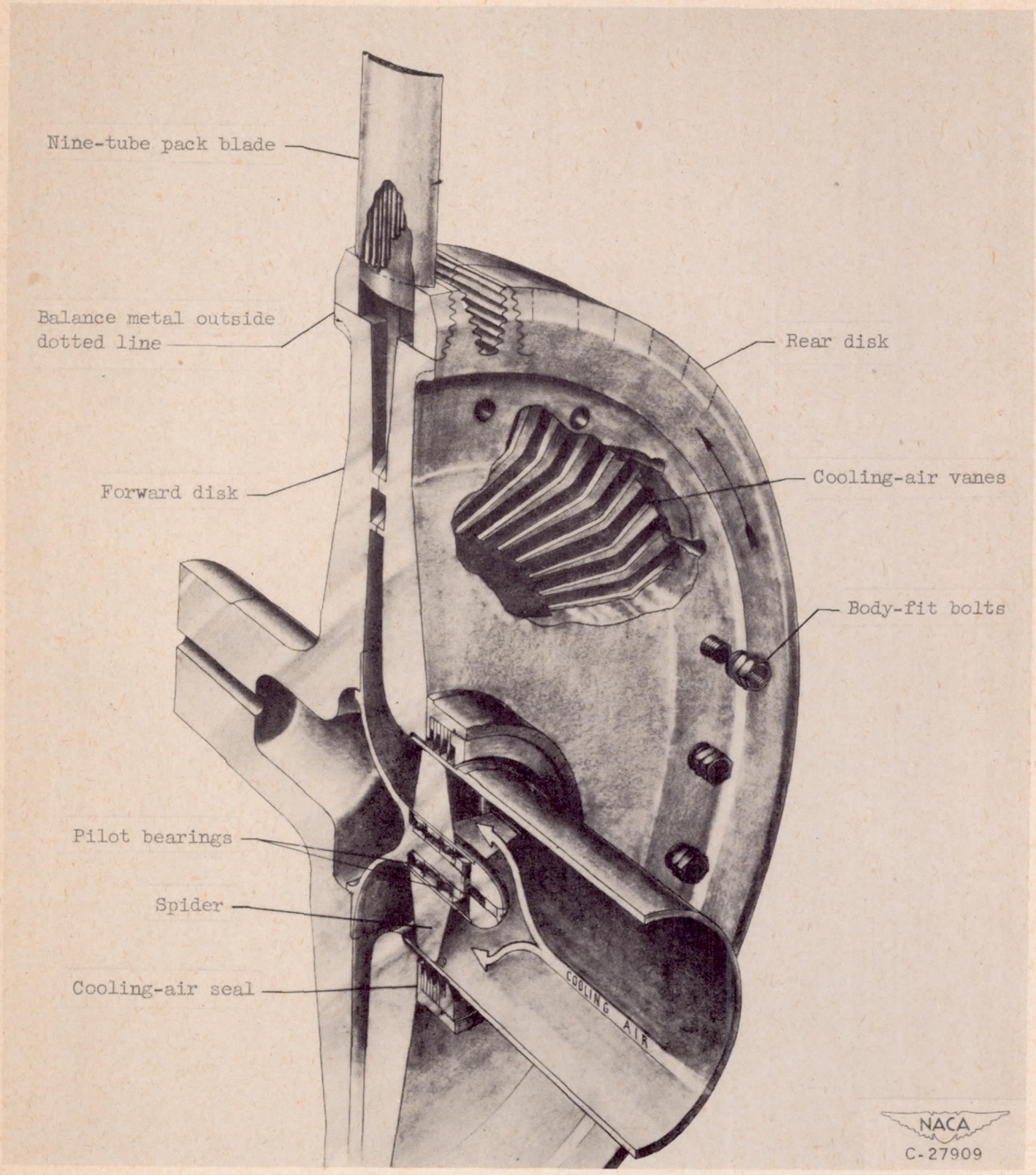

Figure 4. - Air-cooled split rotor with 54 integrally machined vanes.

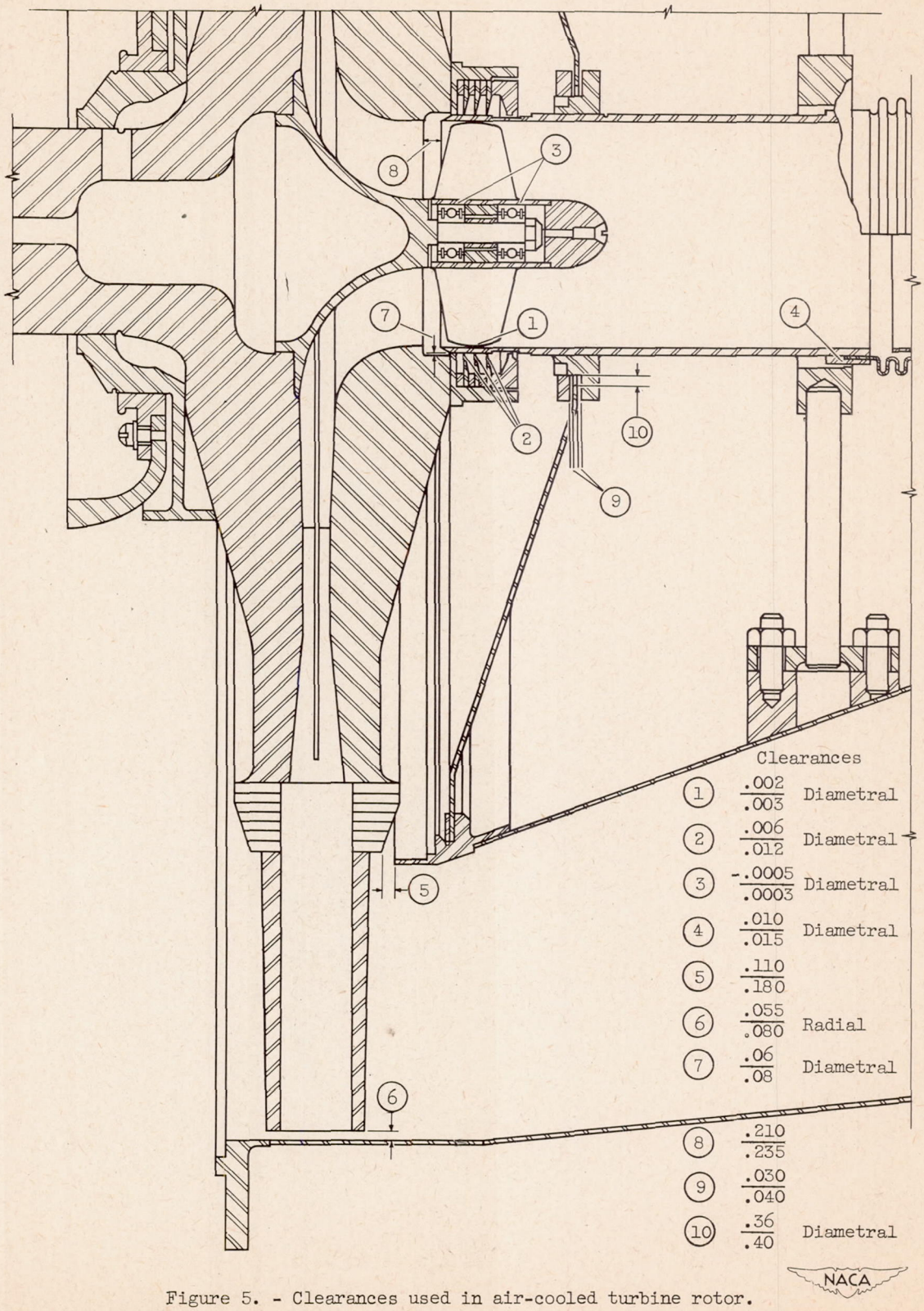

Figure 5. - Clearances used in air-cooled turbine rotor.

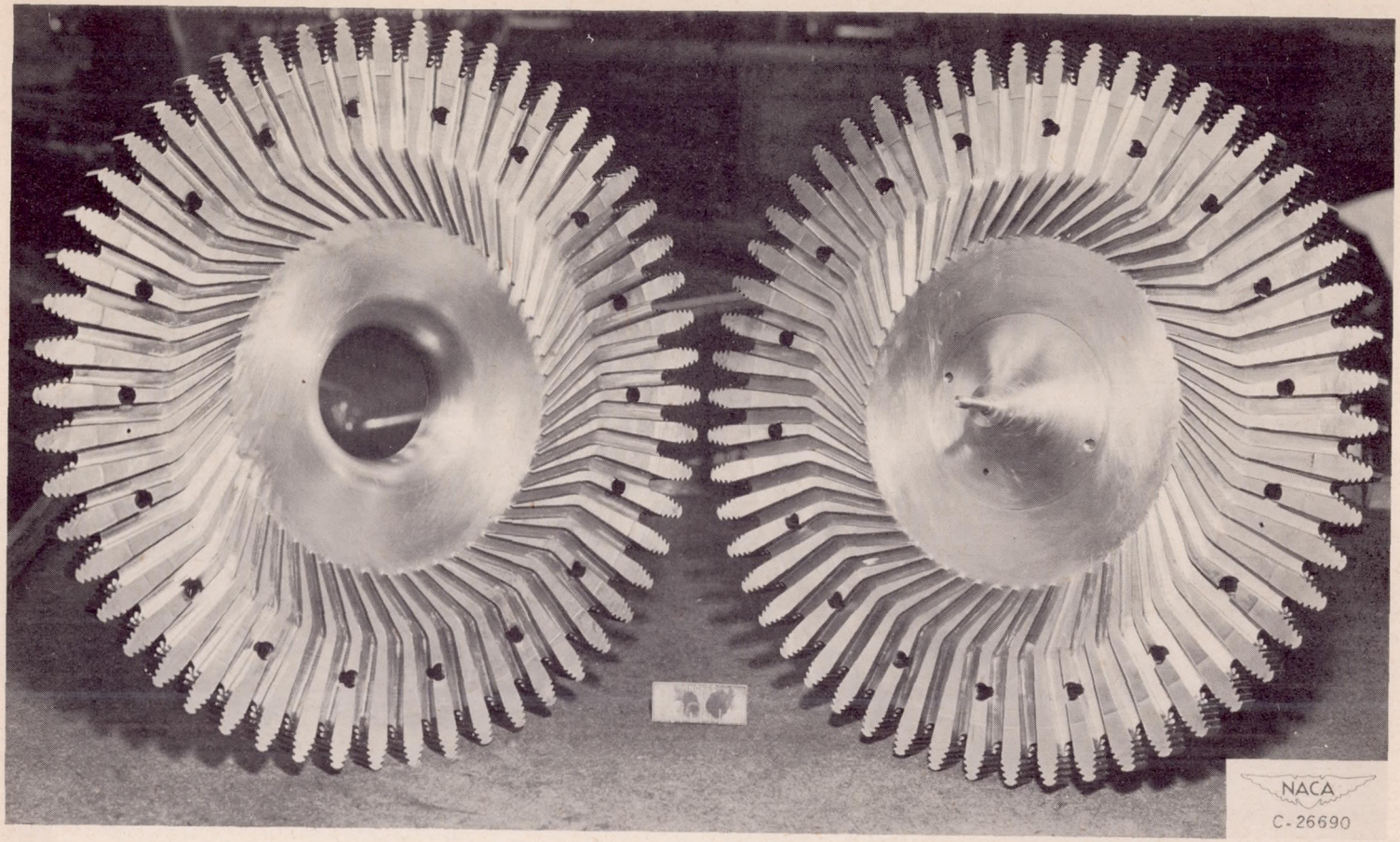

(a) Rear disk (b) Forward disk with pilot bearing spindle in place.

Figure 6. - Photograph showing 54 vanes machined to form cooling-air passage in split rotor for J33 air-cooled turbine.

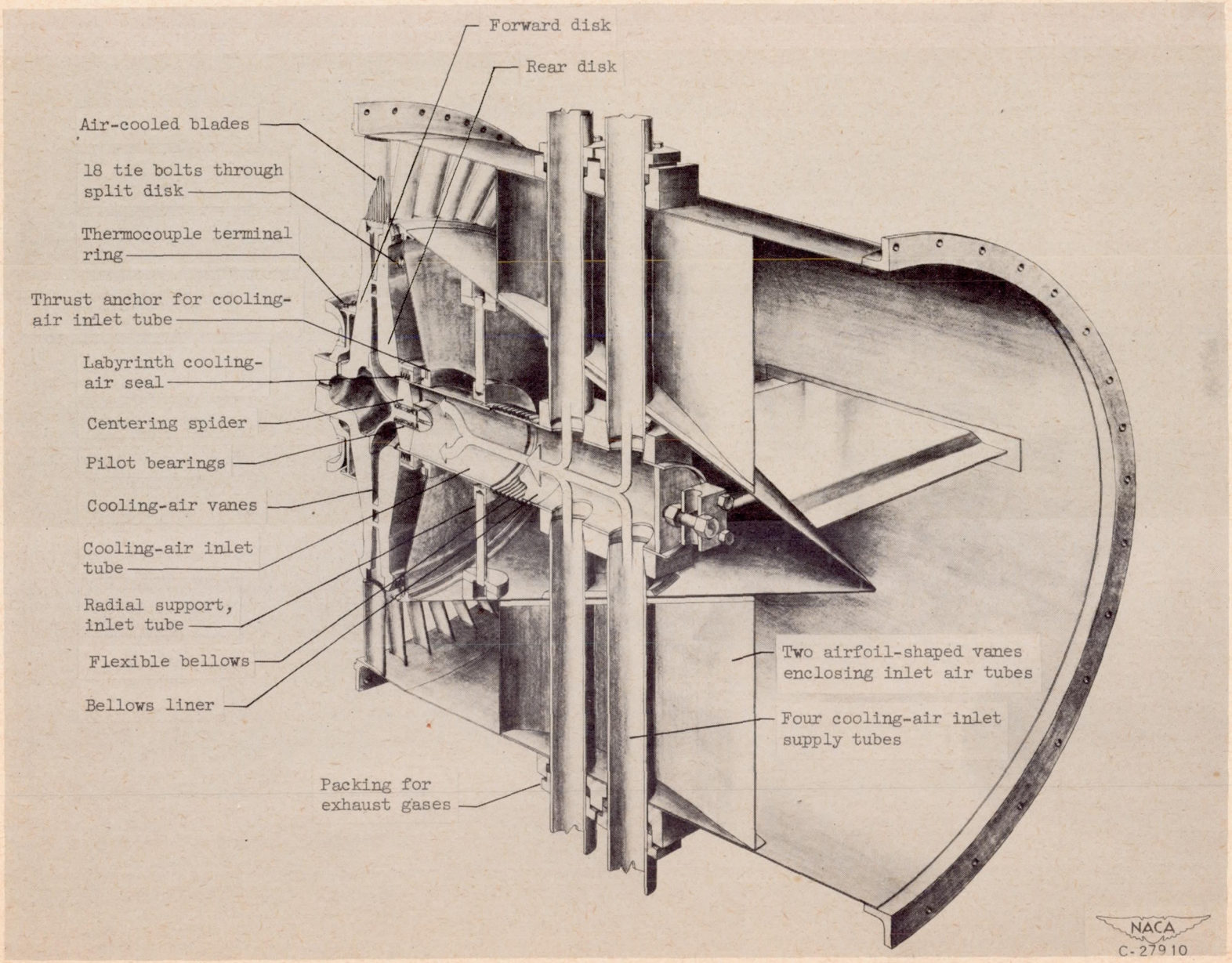

Figure 7. - Assembly of split-rotor, rear-disk cooling-air induction system and tail cone.

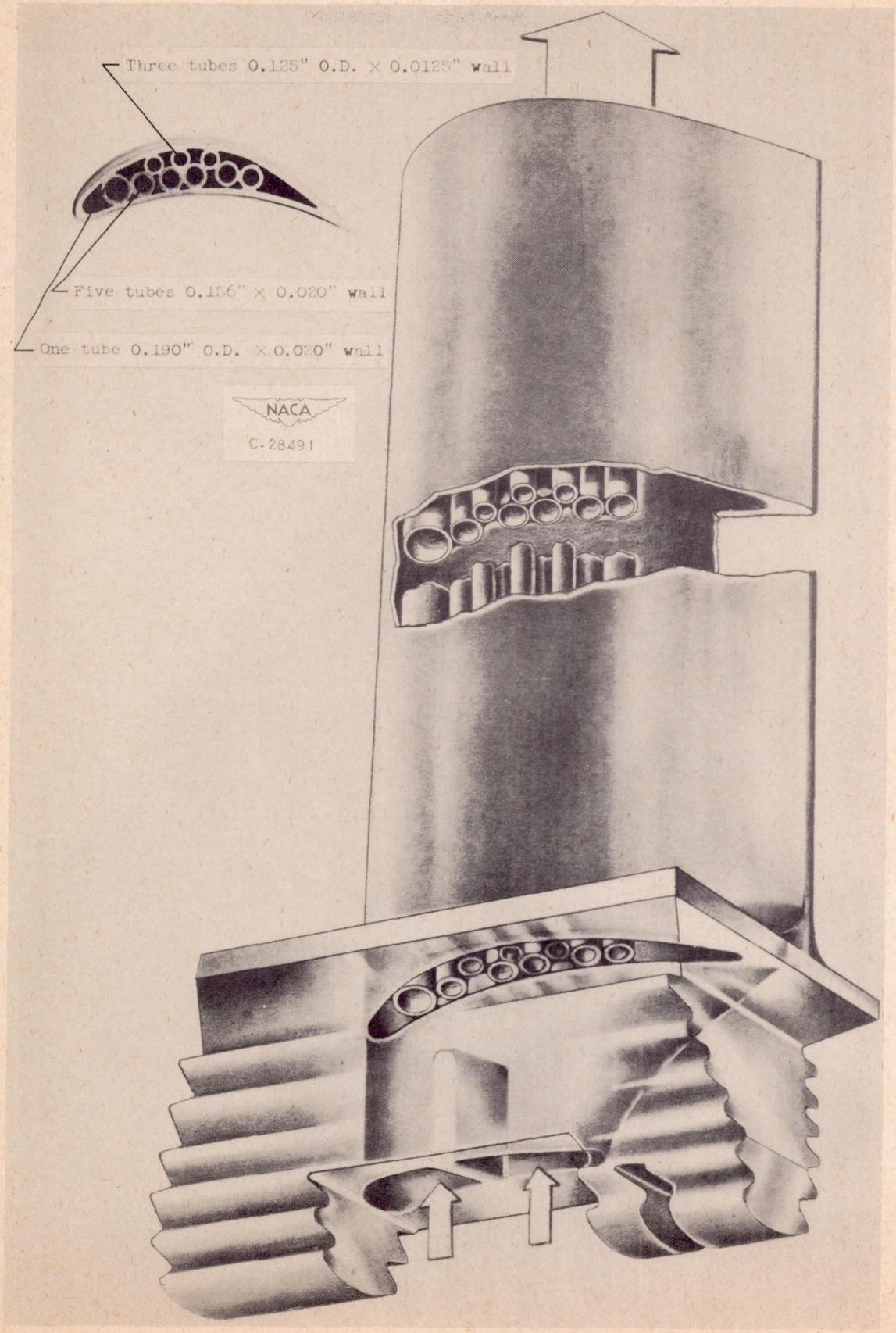

Figure 8. - Nine-tube pack cast X-40 air-cooled blade.

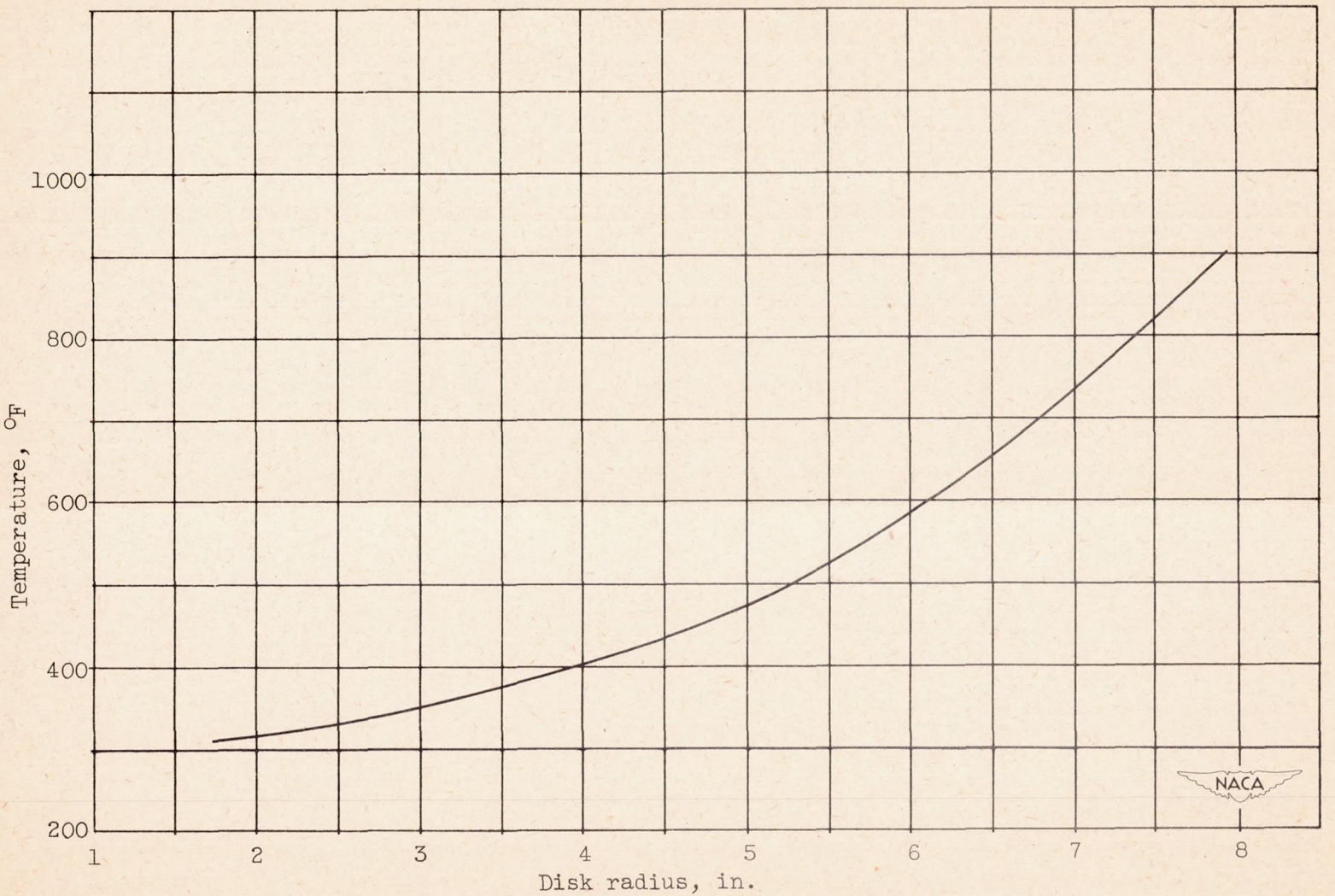

Figure 9. - Assumed disk-temperature variation with radius.

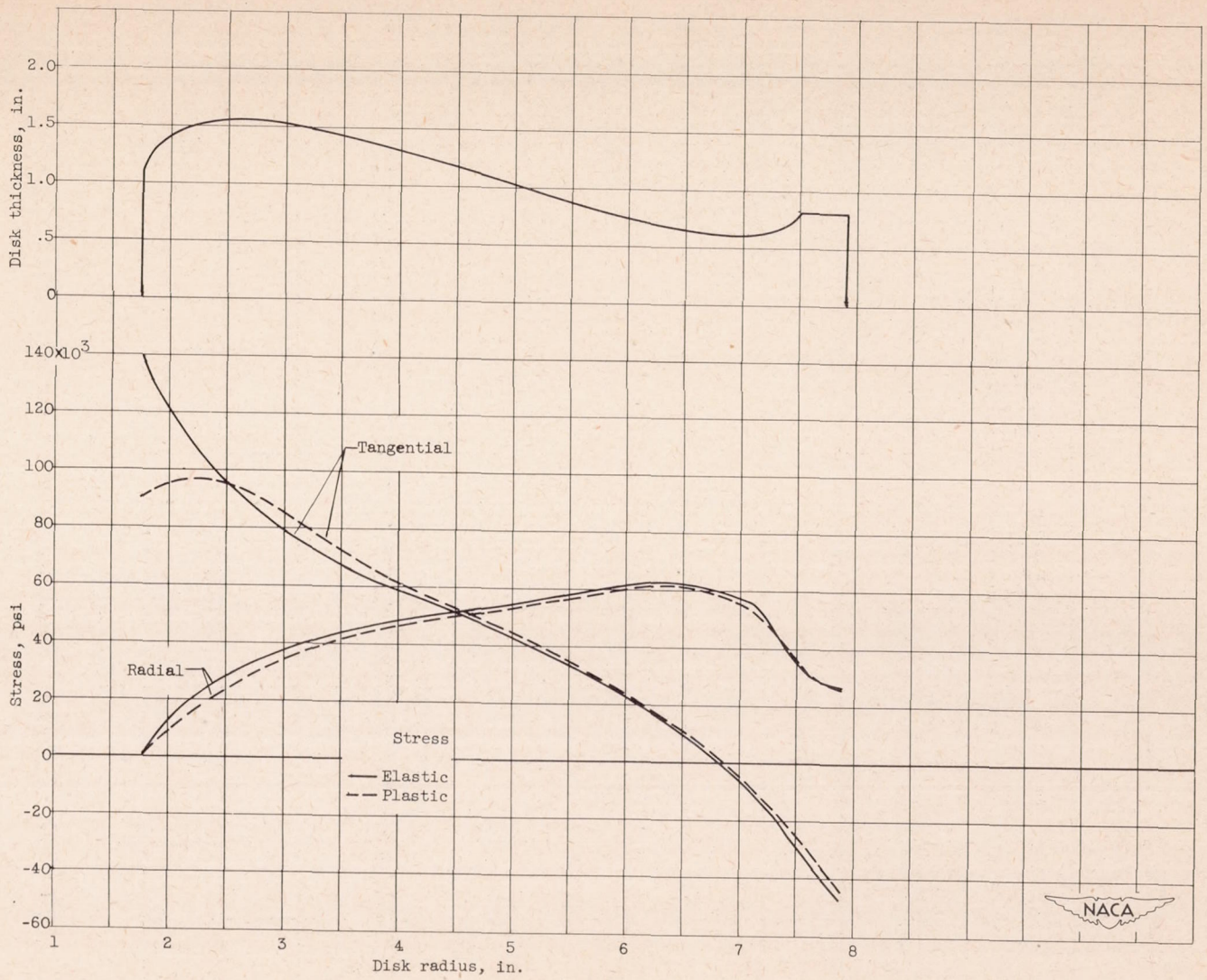

Figure 10. - Effective profile and elastic and plastic stresses at 12,650 rpm for split rotor with assumed radial-temperature gradient.

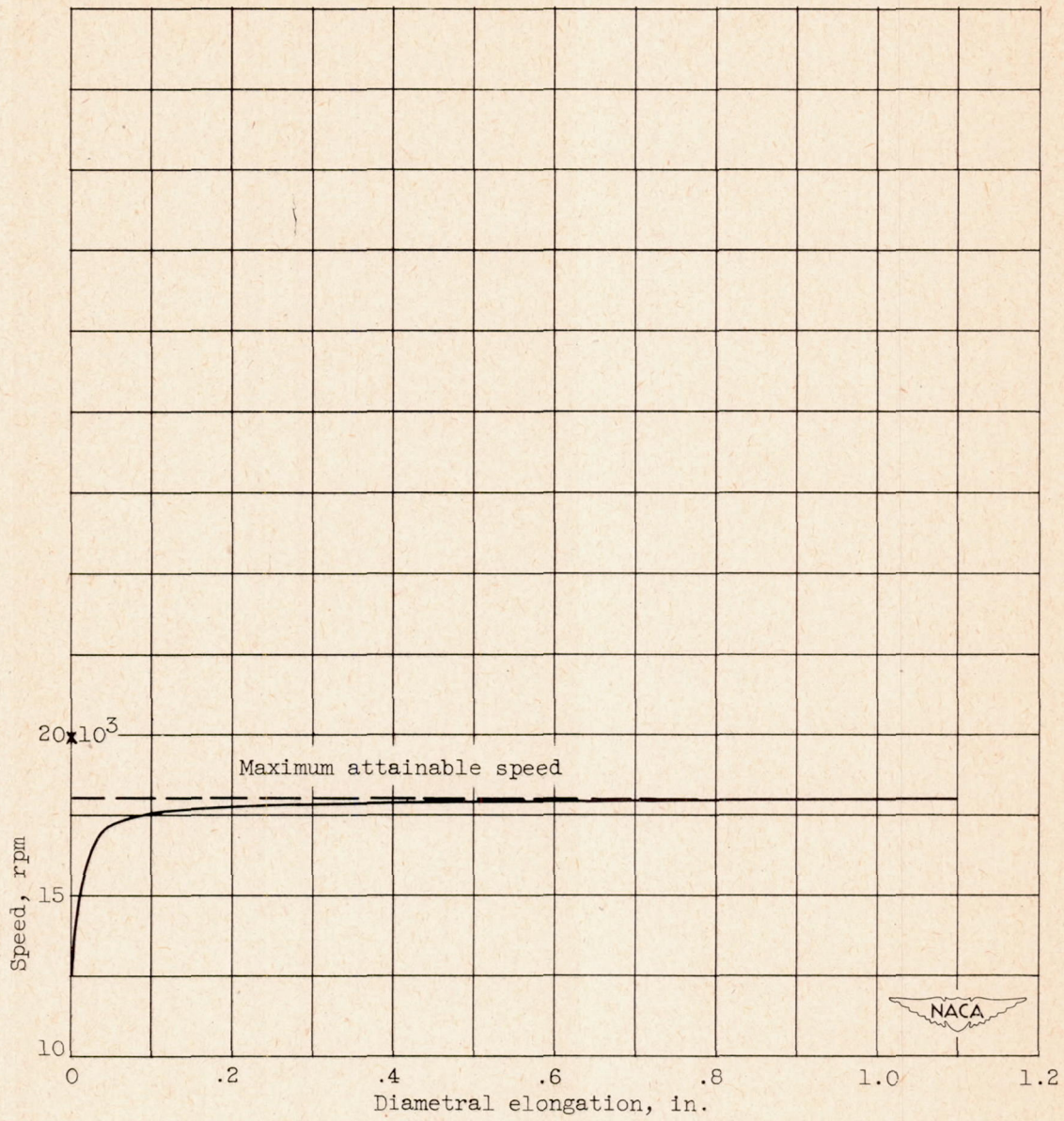

Figure 11. - Deformation and bursting of air-cooled rotor.

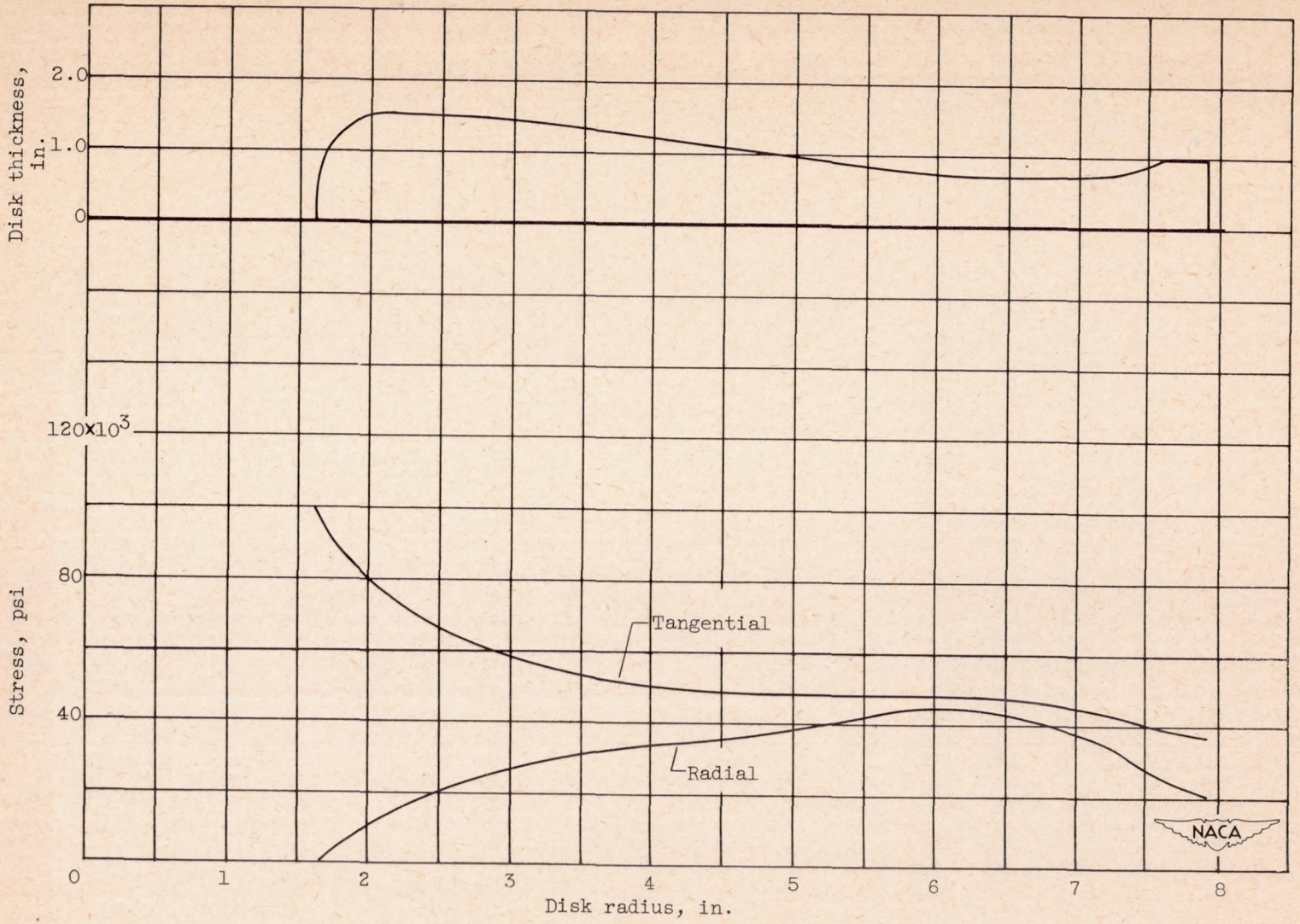

Figure 12. - Effective profile and stresses at 12,650 rpm for split rotor used in spin test.

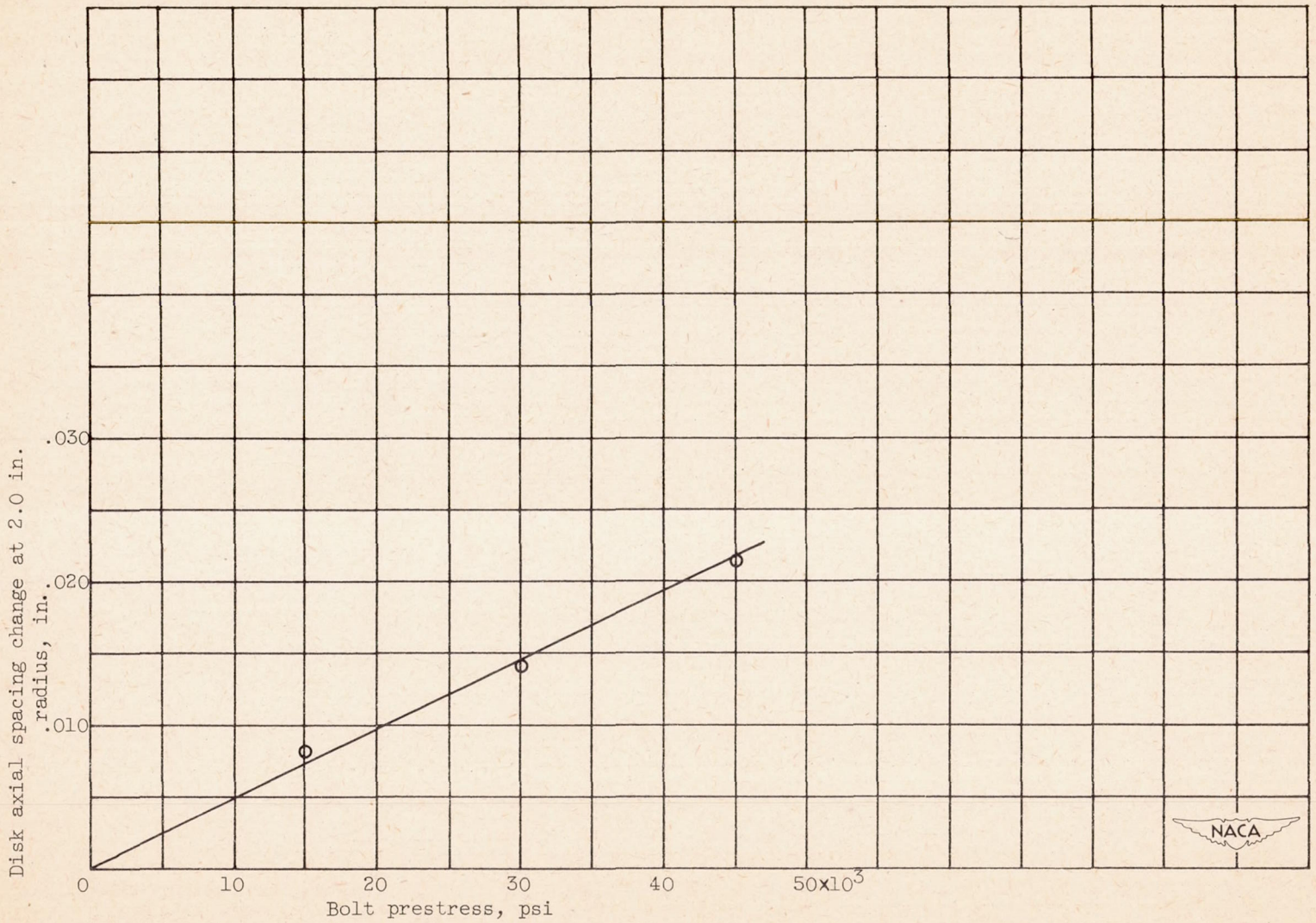

Figure 13. - Relation between bolt prestress and disk axial spacing.

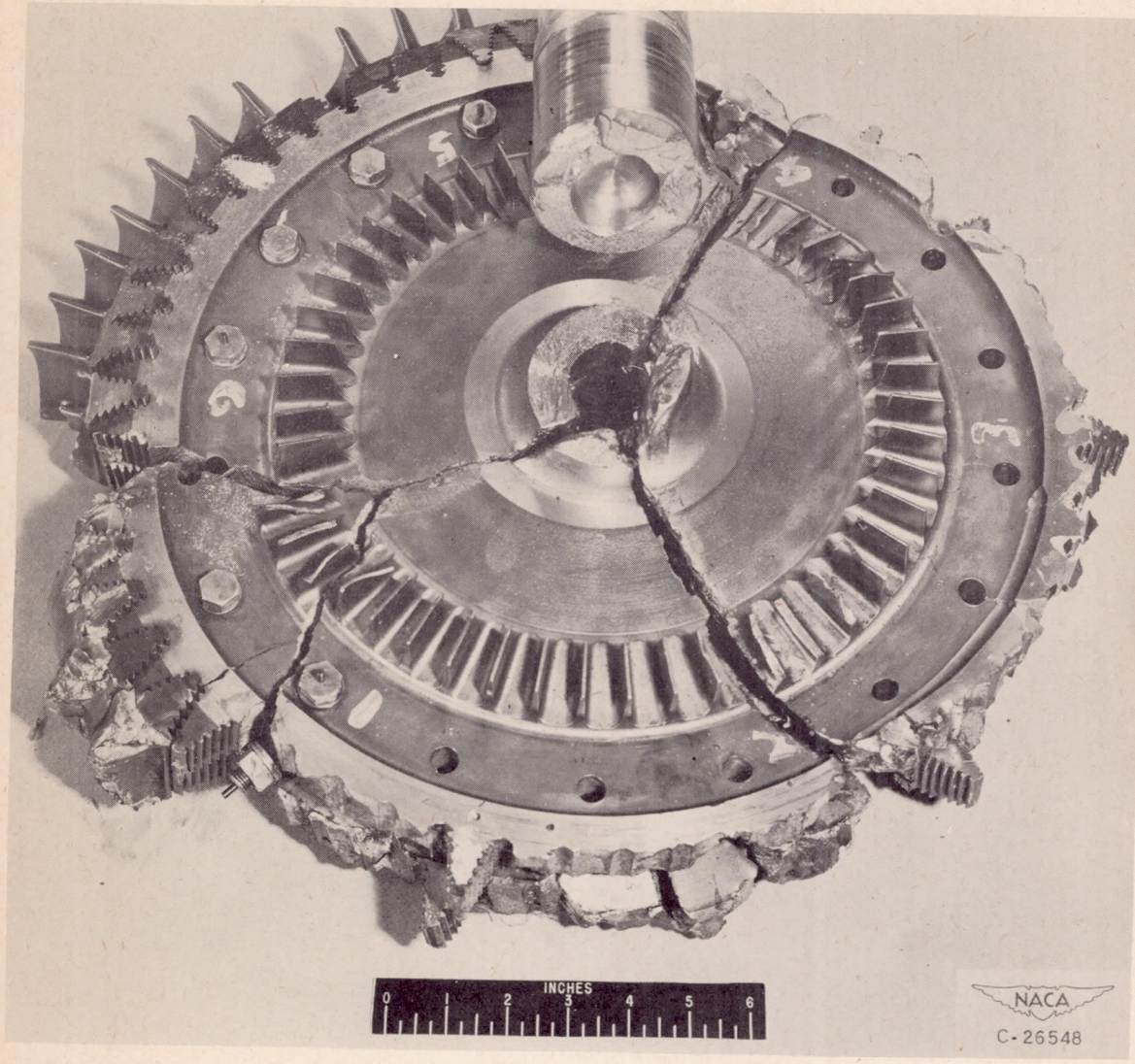

(a) Forward disk fragments and shaft.

Figure 14. - Burst air-cooled rotor.

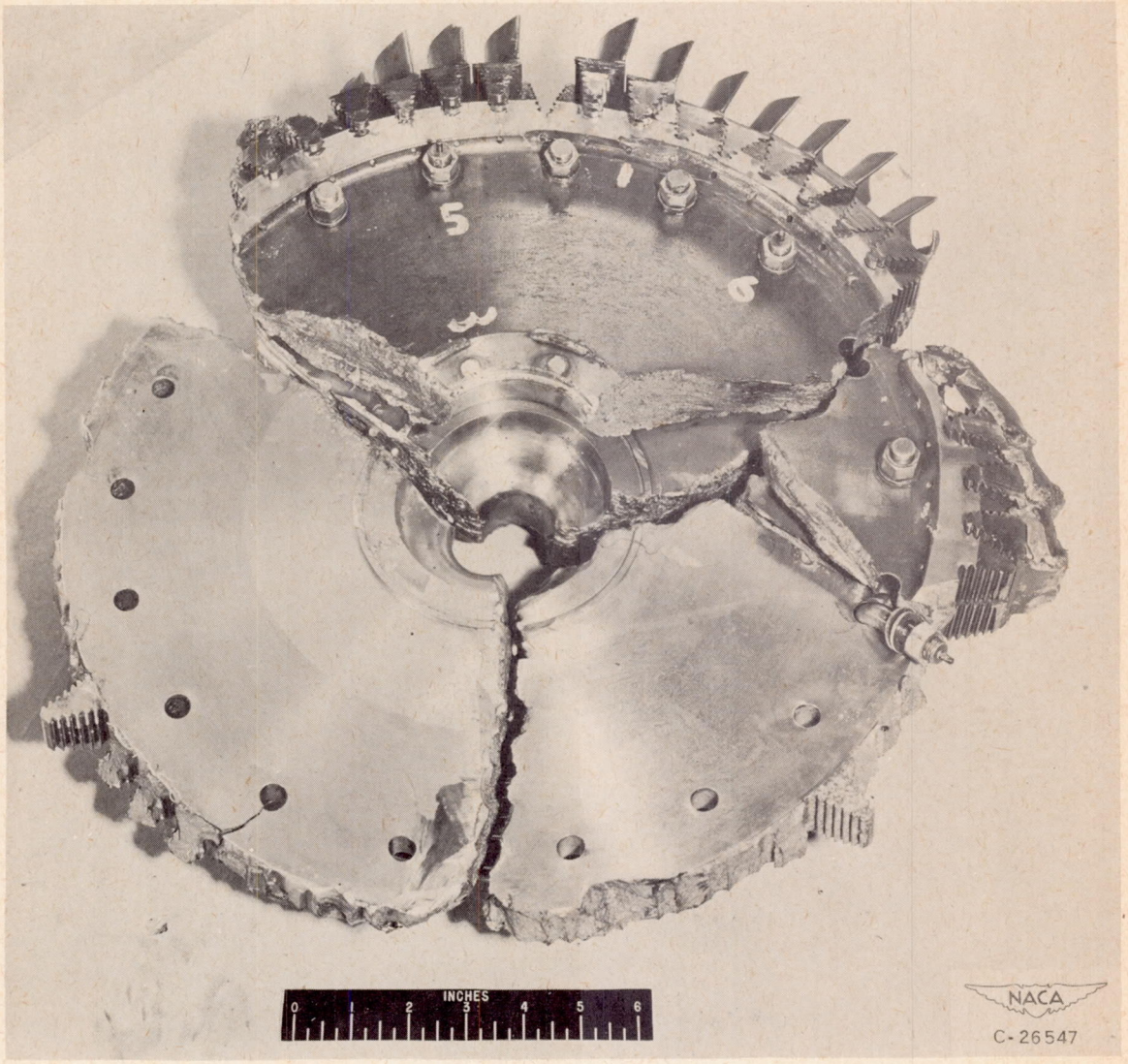

(b) Forward and rear disk fragments viewed from rear side.

Figure 14. - Continued. Burst air-cooled rotor.

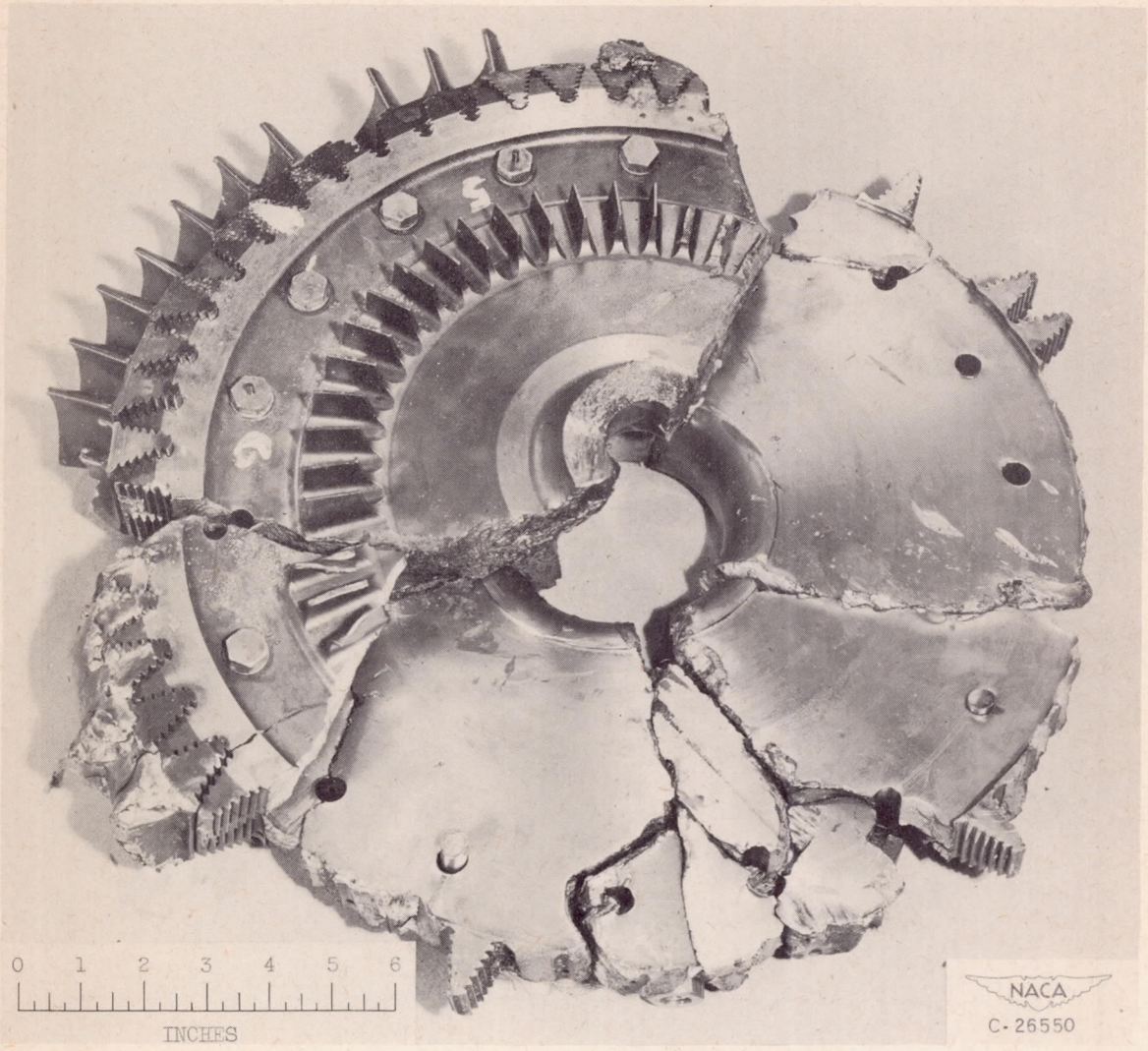

(c) Forward and rear disk fragments viewed from forward side.

Figure 14. - Concluded. Burst air-cooled rotor.

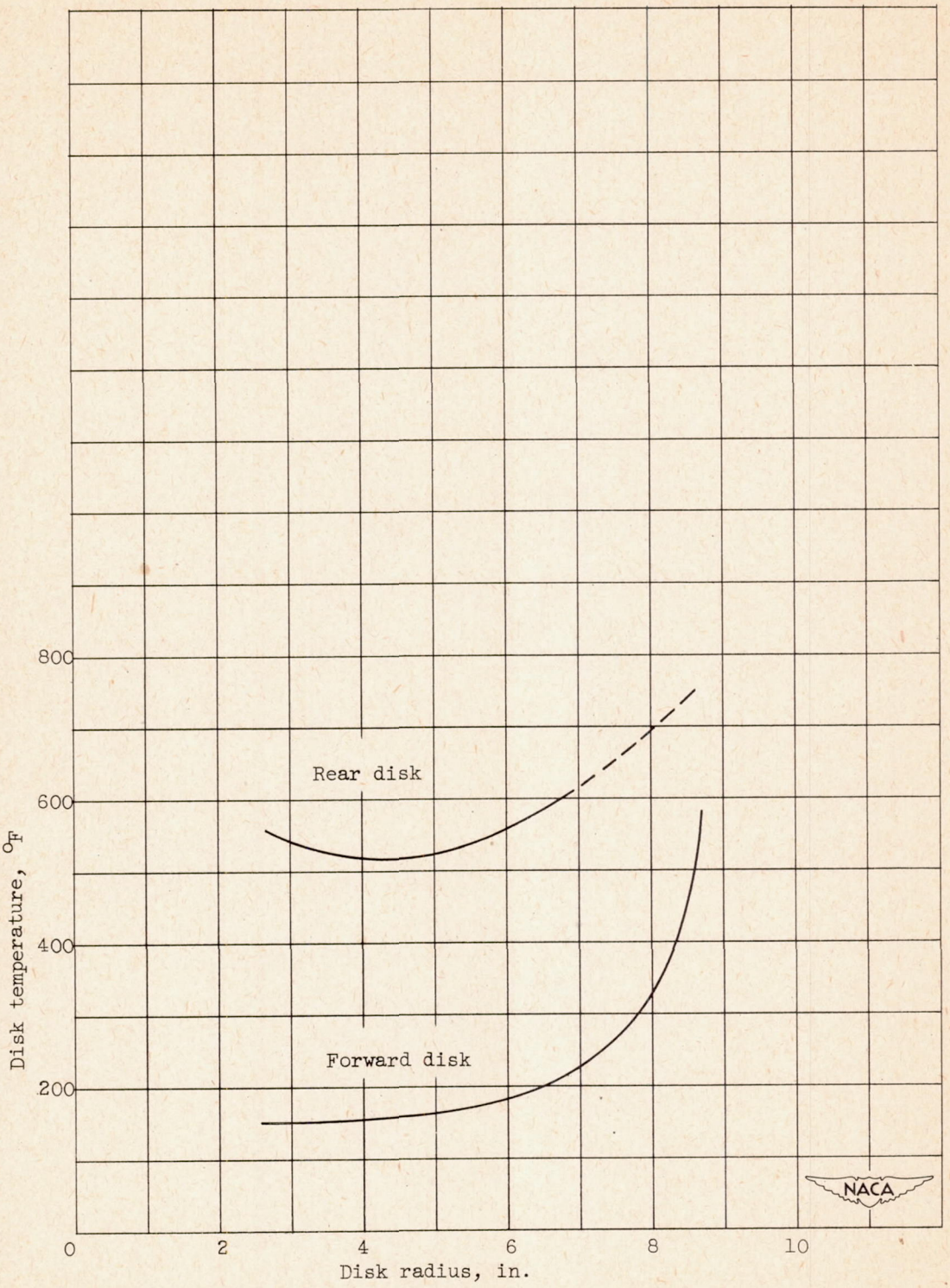

Figure 15. - Disk temperature distributions at 11,500 rpm, based on measured temperatures at lower speeds (reference 1). Engine speed, 11,500 rpm; cooling-air flow ratio, 0.02; cooling-air inlet temperature, 120° F; effective gas temperature, 1445° F.

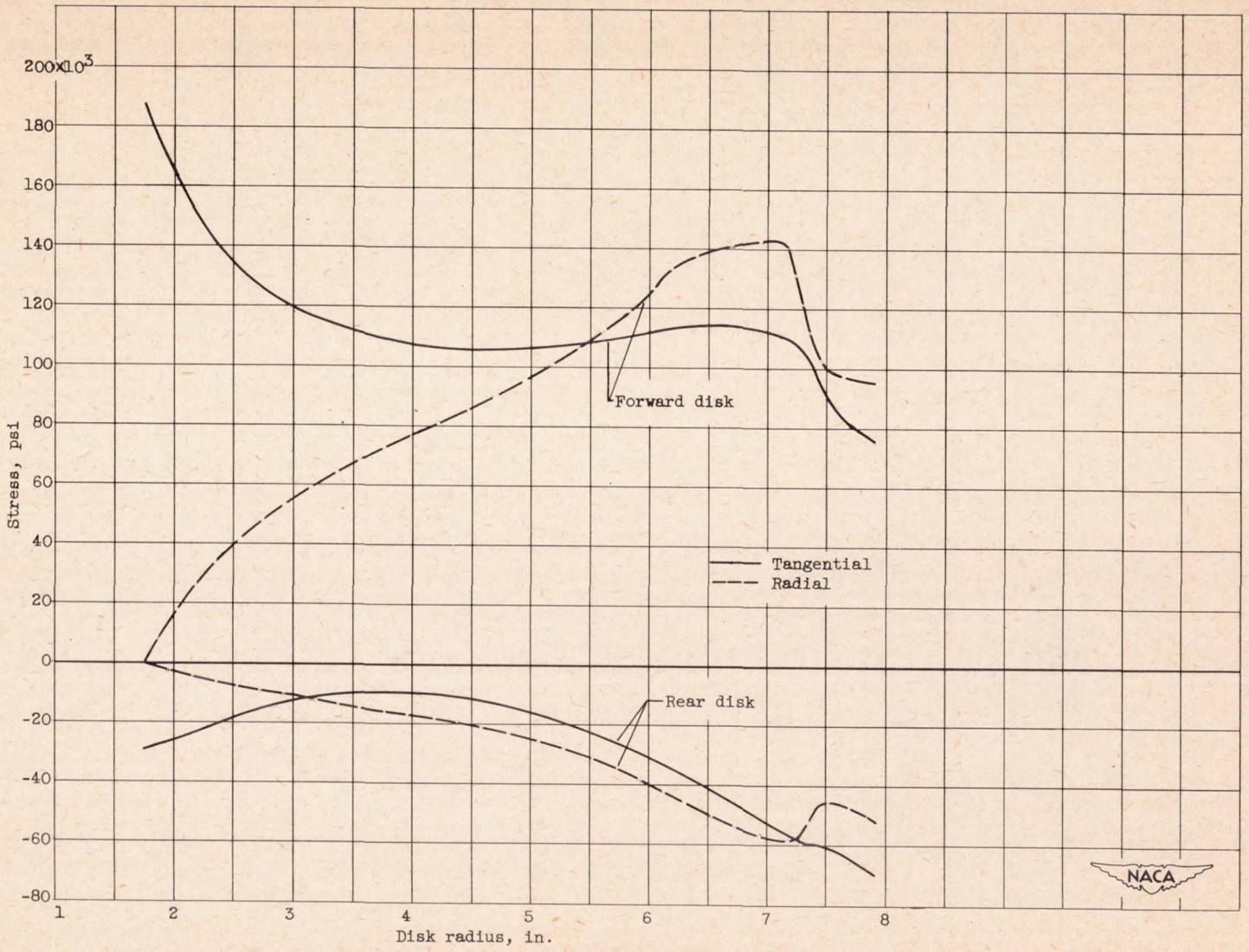

Figure 16. - Elastic stresses for forward and rear disks having dissimilar temperature distributions at 11,500 rpm.

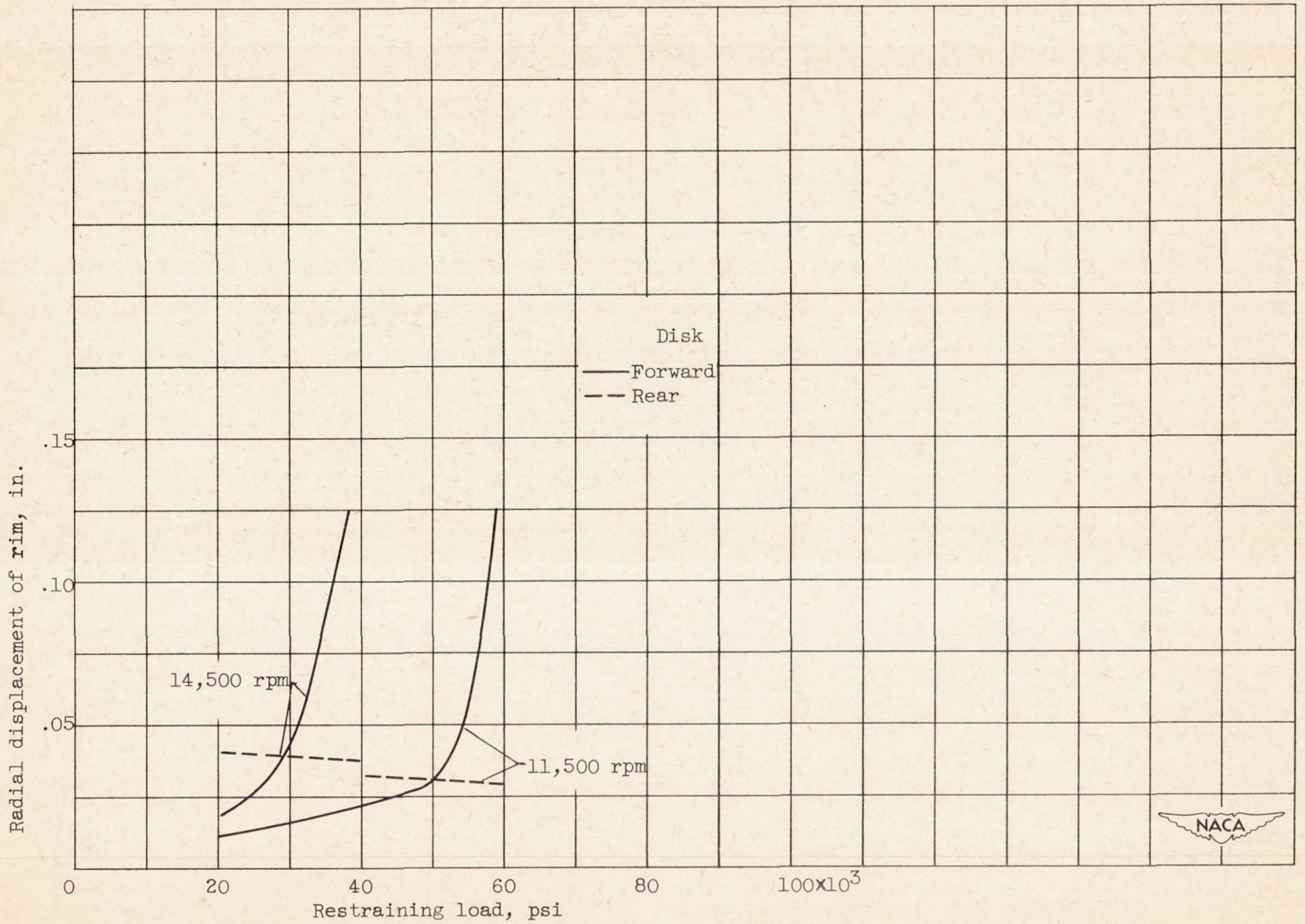

Figure 17. - Graphical determination of restraining loads at 11,500 and 14,500 rpm.

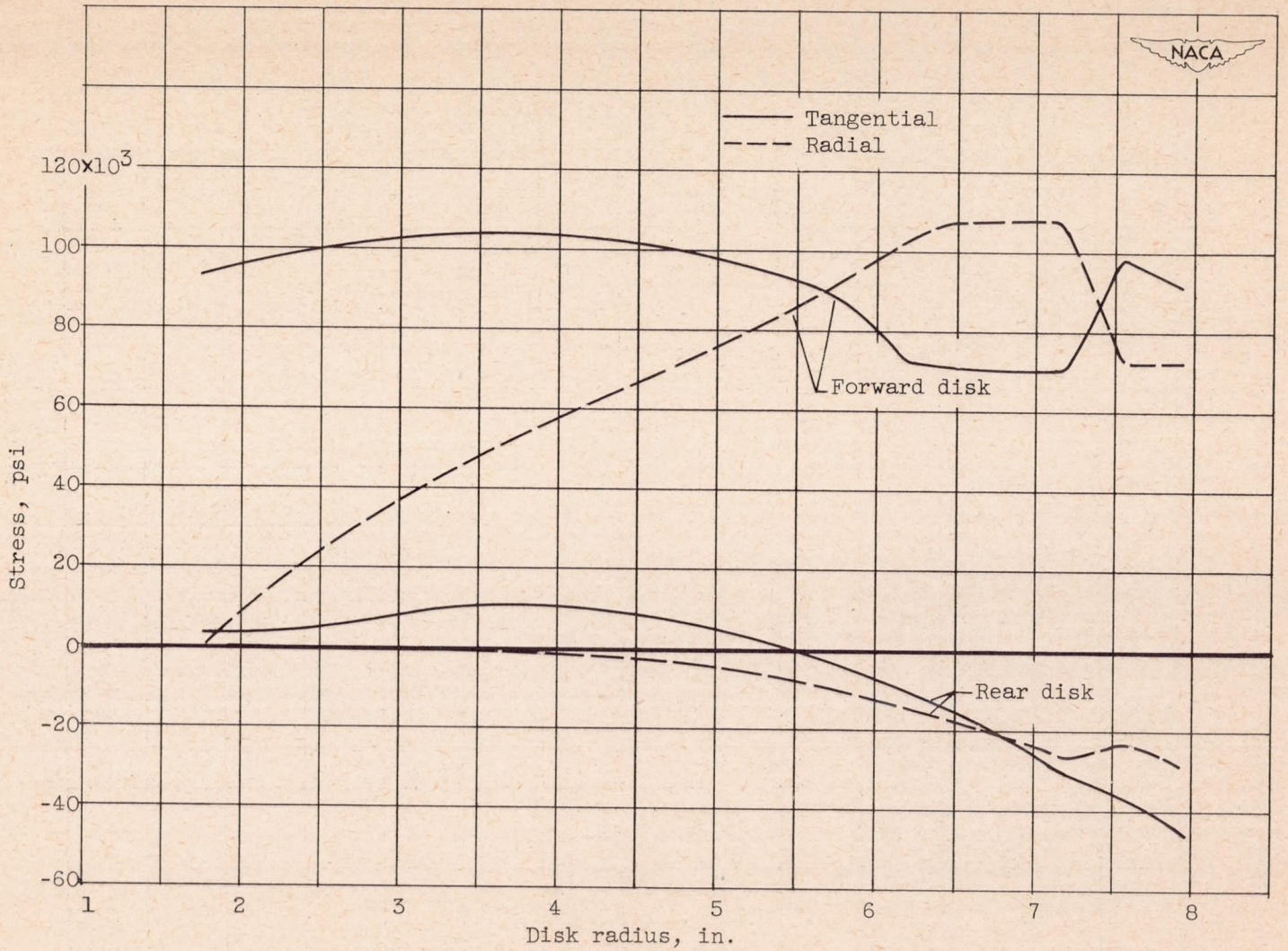

Figure 18. - Plastic stresses for forward and rear disks having dissimilar temperature distributions at 11,500 rpm.

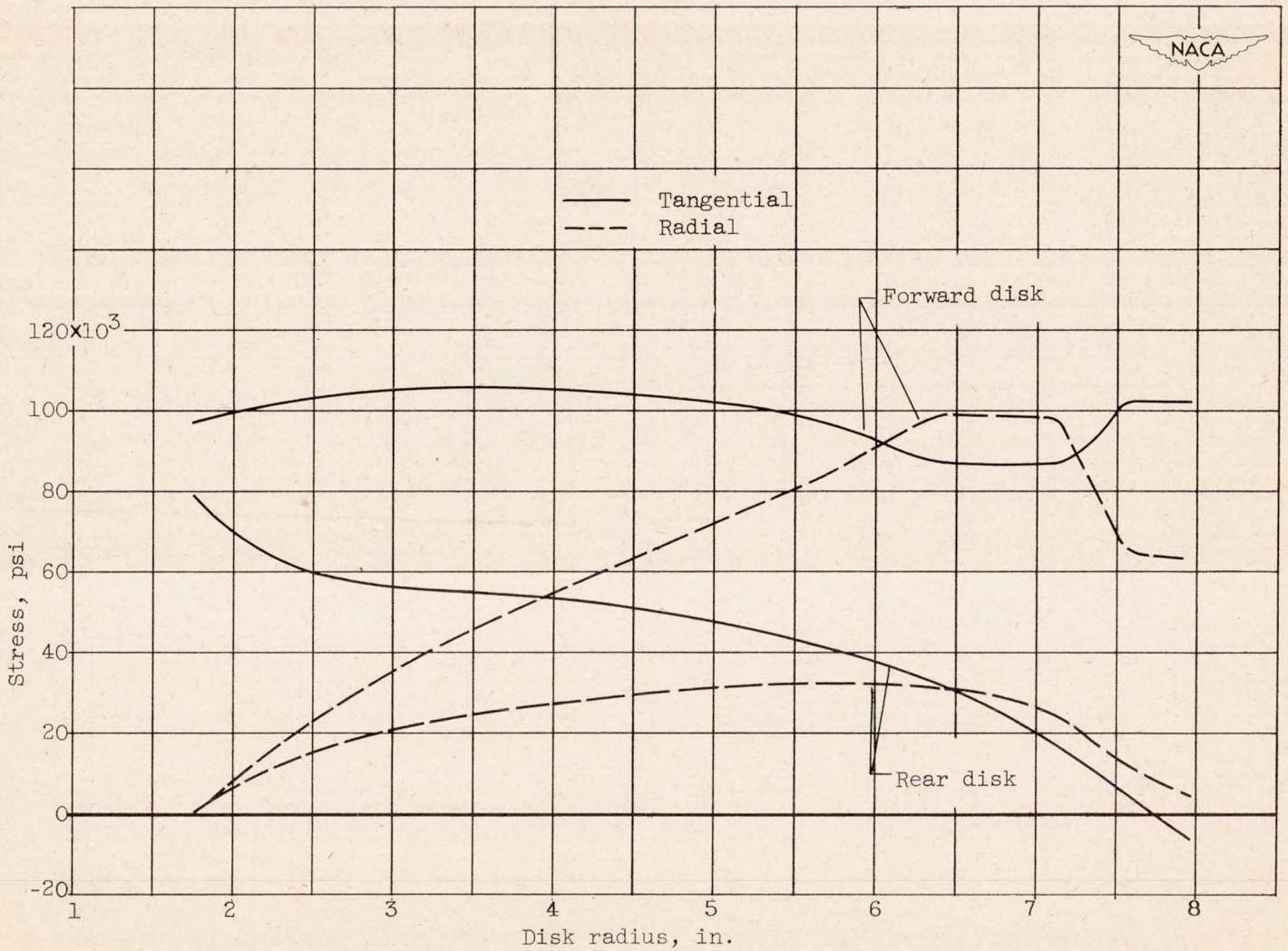

Figure 19. - Plastic stresses for forward and rear disks having dissimilar temperature distributions at 14,500 rpm.